UNIVERSITY OF CALIFORNIA, SAN DIEGO

Bottom up Approach for the Reconstitution and Characterization of DNA Replication Checkpoint

A dissertation submitted in partial satisfaction of the

requirements for the degree Doctor of Philosophy

in

Biology

by

Sheng-hong Chen

Committee in charge:

Professor Huilin Zhou, Chair
Professor Michael David, Co-chair
Professor Richard D. Kolodner
Professor Jean Y. J. Wang
Professor Yang Xu

2008

The dissertation of Sheng-hong Chen is approved, and it is acceptable in quality and form for publication of microfilm and electronically:

_____

_____

_____

_____

Co-chair

_____

Chair

University of California, San Diego

2008

Table of Contents

List of Figures

List of Tables

Acknowledgements

I would first like to acknowledge my advisor, Huilin Zhou for giving me this privilege to do research in his lab where I have developed and matured as a scientist. His patience guided me in the beginning toward a solid training in performing carful experiments and observations. Later in my graduate study, he gives me full freedom and support to conquer the questions in mind. Huilin has been a great mentor and scientist. If anything can be summarized, I think I have learnt from him to address questions in a simple, informative and basic fashion. I feel lucky to have been working with him for the past few years.

I would like to acknowledge the members of my committee who have been keeping me grounded and providing me critical suggestions, and encouragements not only on my research but also on my scientific career. From them, I see the model of great scientists. Of course I have to thank my colleagues, including Claudio Albuquerque, Xiao, Wei, Marcus Smolka, Greg Fuchs, and Sherry Tong. They have been great friends and labmates who have made our days not only endurable but also fun.

I would also like to thank tremendous support I received from all the friends in Ludwig Institution for Cancer Research. In particular, Christopher Putnam, Sharsti Sandall, Marc Mendillo, and Samantha Zeitlin who ever hesitated to take the time to discuss ideas, and experiments I dreamed about. In addition, I also have to thank Kristina H. Schmidt, Brian Orelli, Jorrit Enserink, Scarlet Shell, Joo-Seok Han, Yumi Kim, Daniel R. Foltz, Molly Bush,

and Shuo-Chien Ling who have been helping me through my doctorial research.

I am indebted to my family for their love. They have been continuously supportive of all my decisions. I remember the day I told them I decided to quit my first undergraduate degree, my parents only encouraged me to do what I really want. They have always believed I could achieve anything and wished me follow my heart. Finally, I want to thank my wife, Ying-ja Chen; who has been my friend, teacher, and lover; who always listens to my questions, and problems; who provides me support, advice and answers; who guided me to read my first paper in biochemistry; who drags me out of lab to breath fresh air and surf at beach. I couldn't possibly have completed my dissertation without her.

Chapter 2, in full, was published under the following citation: Chen, S.-H., Smolka, M.B., and Zhou, H. (2007) Mechanism of Dun1 activation by Rad53 phosphorylation in Saccharomyces cerevisiae. Journal of Biological Chemistry 282, 986-995. The dissertation author was the primary researcher and author of this paper.

Vita

1998 BS, Zoology, National Taiwan University, Taiwan

2001 MS(Distinction), Evolutionary and Adaptive System, University of Sussex

2008 PhD, Biological Sciences, University of California, San Diego

Publications

Smolka, M.B., Albuquerque, S.P., **Chen, S.-H.**, Schmidt, K.H., Wei, X.X., Kolodner, R.D., and Zhou, H. (2005) Dynamic Changes in Protein-protein Interaction and Protein Phosphorylation Probed with Amine Reactive Isotope Tag. Molecular and Cellular Proteomics 4, 1357-1369.

Su, Y.H., **Chen S.-H.**, Zhou, H, and Vacquier, V.D. (2005) Tandem mass spectrometry identifies proteins phosphorylated by cyclic AMP-dependent protein kinase when sea urchin sperm undergo the acrosome reaction. Dev Biol 285, 116-125.

Smolka, M.B., **Chen, S.-H.**, Maddox, P.S., Enserink, J.M., Albuquerque, C.P., Wei, X.X., Desai, A., Kolodner, R.D., and Zhou, H. (2006) An FHA domain mediated protein interaction network of Rad53 reveals its role in the regulation of polarized cell growth. Journal of Cell Biology, 175, 743-753.

Chen, S.-H., Smolka, M.B., and Zhou, H. (2007) Mechanism of Dun1 activation by Rad53 phosphorylation in Saccharomyces cerevisiae. Journal of Biological Chemistry, 282, 986-995.

Smolka M.B., Albuquerque C.P., **Chen, S.-H.**, and Zhou, H. (2007) Proteome-wide identification of in vivo targets of DNA damage checkpoint kinases. PNAS 104, 10364-10369.

ABSTRACT OF THE DISSERTATION

Bottom up Approach for the Reconstitution and Characterization of DNA Replication Checkpoint

by

Sheng-hong Chen

Doctor of Philosophy in Biology

University of California, San Diego, 2008

Professor Huilin Zhou, Chair

Professor Michael David, Co-chair

Faithful genome duplication is fundamentally important for all organisms. When cells encounter DNA replication stress, from difficulties in replicating either repeated sequence or aberrant DNA structure resulting from UV radiation or genotoxic chemicals, replication forks are stalled. This impediment may result in the collapse of replication forks and consequently

DNA damage. Eukaryotes have evolved a signaling pathway, namely DNA replication checkpoint, which regulates cellular responses for cell viability and maintenance of genome stability under replication stress. Defects in replication checkpoint results in genomic instability, cell death and cancer.

Activation of effector kinases is the hallmark of DNA replication checkpoint. They are responsible for coordinating many cellular responses after replication stress, ranging from the stabilization of stalled replication forks to the cell cycle arrest. While the functions of the effector kinases have long been appreciated, the molecular mechanisms for their activation remain elusive. Studies presented here, which utilize the biochemical and genetic amenability of budding yeast, *Saccharomyces cerevisiae*, reveal the molecular basis of effector kinases activation.

Discoveries in Chapter 2 showed the reconstitution of the activation and phosphorylation state of an effector kinase, Dun1. Analysis on its phosphorylation reveals the specific phosphorylation on its activation loop that triggers it activation. Additionally, this specific residue at the activation loop of all Chk2 family kinases are conserved. We thus suggested this activation loop phosphorylation to be a conserved regulation for the activation of Chk2 family kinases, including Dun1 and Rad53 in budding yeast.

Mrc1, as part of replication machinery, serves as a docking site at stalled replication fork for the recruitment of another effector kinase Rad53. Mec1, a PIKK kinase, is the upstream replication checkpoint sensor. Both

Mec1 and Mrc1 have been implicated to be crucial for Rad53 activation. Based on the studies in Chapter2, a biochemical approach using the reconstitution of Rad53 activation has led to the discovery of efficient Rad53 activation by Mec1 mediated through Mrc1. Analysis on the reconstituted system showed that instead of a two-step linear pathway, the primary role of Mrc1 is to promote Rad53 phosphorylation by Mec1 by catalyzing the enzyme-substrate interaction between Mec1 and Rad53.

Chapter 1: Introduction

1.1 DNA replication checkpoint

Faithful replication of the genome is important for all organisms. During DNA replication, errors could arise from a variety of courses, including intrinsic errors made by DNA polymerases, difficulty in replicating repeated DNA sequences, or failure to repair damaged DNA caused by either endogenous oxidative agent or exogenous mutagens such as UV and DNA damaging chemicals (Neecke et al., 1999; Samadashwily et al., 1997). Under these circumstances, the evolutionarily conserved DNA replication checkpoint is activated and helps multiple processes to stabilize replication forks, block late origin firing and delay mitosis in cells under replication stress, and to ultimately recover from replication blocks (Desany et al., 1998; Lopes et al., 2001; Santocanale and Diffley, 1998; Tercero and Diffley, 2001; Tourriere et al., 2005; Weinert et al., 1994). Defects in the DNA replication checkpoint signaling could result in genomic instability, cancer development and cell death (Hartwell and Kastan, 1994; Myung et al., 2001; Tercero et al., 2003).

1.1.1 Checkpoint sensors and effectors

Genetic studies in budding yeas *S. ceravisiae* have been successfully identified many players in the DNA replication checkpoint. Mec1, an ortholog of human ATR, is a phosphoinositide 3-kinase-like kinase (PIKK) in *S.*

ceravisiae that involves in sensing DNA replication stress. Mec1 forms a complex with Ddc2 (ortholog of human ATRIP) and the Mec1-Ddc2 complex is recruited to stalled replication forks through RPA-coated single-stranded DNA, which is an integral part of DNA replication fork (Katou et al., 2003; Sogo et al., 2002; Zou and Elledge, 2003). Mec3-Rad17-Ddc1 (9-1-1) complex, a PCNA-like checkpoint clamp, is loaded to single and double stranded DNA junction of the stalled replication forks through the clamp loader Rad24-RFC complex (Katou et al., 2003; Majka and Burgers, 2003). While Mec1 and checkpoint clamp/clamp loader are mainly responsible for the sensing of replication stress, the effector kinases Rad53 and Dun1, the Chk2 family kinases, are the major downstream kinases that coordinate many cellular responses including the stabilization of replication forks, block late origin firing, up-regulation of dNTP level for DNA repair, and cell cycle arrest (Lopes et al., 2001; Santocanale and Diffley, 1998; Weinert et al., 1994; Zhao and Rothstein, 2002).

1.1.2 Replication machinery involved in replication checkpoint

Aside from replicating the genome, components of the DNA replication machinery also appear to participate in the DNA replication checkpoint. Increasing number of proteins has been shown to have dual functions both in DNA replication and checkpoint activation. Mrc1 (for mediator of replication checkpoint) was identified to be important for cells to respond to hydroxyurea in *S. ceravisiae* and *S. pombe* (Alcasabas et al., 2001; Tanaka and Russell,

2001). It associates with the DNA replisome during normal DNA synthesis and travels with replication forks along chromosome (Gambus et al., 2006; Lou et al., 2008; Szyjka et al., 2005). Deletion of MRC1 causes defects in DNA replication suggesting its role in normal DNA replication (Szyjka et al., 2005). Interestingly, when DNA replication is blocked by hydroxyurea, Mrc1 undergoes Mec1 dependent phosphorylation. Mutations of the Mec1 canonical SQ/TQ phosphorylation sites of Mrc1 abolished hydroxyurea induced Mrc1 phosphorylation by Mec1 suggesting a direct phosphorylation of Mrc1 by Mec1 (Alcasabas et al., 2001; Tanaka and Russell, 2001; Xu et al., 2006). Phosophorylated Mrc1 binds to Rad53 and this binding is essential for the kinase activation, which indicate its role in mediating the activation of effector kinases.

Dbp11 and its functional homolog TobBP1 in vertebrates are essential component of replisome (Garcia et al., 2005). Other than the involvement of the initiation of DNA replication, they associate with 9-1-1 complex. In vitro studies in yeast and vertebrate showed its ability to stimulate Mec1/ATR catalytic activity, possibly through binding induced conformational change (Araki et al., 1995; Kamimura et al., 1998; Kumagai et al., 2006; Lee et al., 2007; Navadgi-Patil and Burgers, 2008; Wang and Elledge, 2002). Sgs1 is a helicase that coordinate replication and recombination events during S phase and is important for maintaining genomic integrity (Watt et al., 1996). At the same time, Sgs1's binding to the Rad53 FHA1 motif directly helps the

activation of effector kinase Rad53. Interestingly, Sgs1's catalytic function as a helicase is not required for its ability to activate Rad53 (Bjergbaek et al., 2005). Tof1 is critical for DNA replication forks to pause at diverse chromosomal sites where nonnucleosomal proteins bind very tightly to DNA (Hodgson et al., 2007). Double deletion of RAD9 (a gene involved in G1 and G2/M checkpoint) and TOF1 results in the synergistic defects in Rad53 activation and cellular responses to genotoxic agents such as hydroxyurea and UV radiation (Foss, 2001). POLII, is the gene encoding the catalytic subunit of the third nuclear DNA polymerase and is required for DNA replication (Morrison et al., 1990). pol2 mutants were genetically identified to be defective for the S phase checkpoint (Navas et al., 1995). Pol2 interacts has recently been shown to interact with Mrc1 and this interaction may involve in regulating the S phase checkpoint response to DNA damage on the leading strand (Lou et al., 2008).

1.2 Regulation of replication checkpoint activation

Other than the location of DNA replication, the replication fork also provides a platform to assemble specific signaling molecules in the DNA replication checkpoint, and this assembly of multiple complexes is tightly associated with efficient activation of checkpoint signaling pathway.

1.2.1 Protein-protein interaction mediated activation

Protein-protein interaction appears to be a key regulation in determining the specificity of kinase signaling in replication checkpoint. Upon the activation of replication checkpoint, Mec1-Ddc2 complex is localized to stalled replication fork through its binding to RPA coated single stranded DNA (Sogo et al., 2002; Zou and Elledge, 2003). The relocalization of Mec1-Ddc2 to stalled replication fork may contribute to the activation of replication checkpoint through a localized high concentration of Mec1-Ddc2 and stronger association between Mec1-Ddc2 complex with its activators and substrates (Lee et al., 2007; Majka et al., 2006). Mrc1 has been shown to be a potential substrate of Mec1. Its phosphorylation state change after replication stress is Mec1 dependent (Alcasabas et al., 2001). Phosphorylated Mrc1 recruits Rad53 through its phosphorylated motif binding to Rad53 FHA domain. Recruited Rad53 may therefore undergo direct Mec1 phosphorylation on its N-terminal TQ sites (Lee et al., 2003). In *S. pombe*, it has been suggested that phosphorylated N-terminal TQ sites could cause oligomerization of Cds1 through FHA domain binding in trans, and then lead to the auto-activation of Cds1 (Xu et al., 2006). Although if the exact mechanism can promote Rad53 auto-activation remains to be unclear to us. In addition to the potential role of mediating auto-activation, phosphorylated N-terminal TQ sites of Rad53 has been indicated to bind to Dun1 FHA domain and consequently results in Dun1 activation (Chen et al., 2007; Lee et al., 2003). This chain of protein-protein interactions

initiated from Mel-Ddc2 phosphorylation of Mrc1 may greatly determine the specificity of kinase signaling cascade.

1.2.2 Activation through the stimulation of catalytic activity

Studies in *Xenopus laevis* implicated that the immunoprecipitated ATR after replication stress has higher activity (Guo et al., 2000; Kumagai et al., 2004), which suggested its modification or associated factors are contributing to its higher activity. With purified protein, TopBP1 and Dpb11 have been shown to directly stimulate ATR and Mec1 activity in vitro in *X. laevis*, and *S. ceravisiae* respectively (Kumagai et al., 2006; Mordes et al., 2008; Navadgi-Patil and Burgers, 2008). This stimulation of ATR activity is associated with a stronger enzyme-substrate interaction, possibly due to TopBP1 induced ATR conformational change (Mordes et al., 2008).

9-1-1 complex and its loader Rad24-RFC has been shown to stimulate Mec1 activity in vitro. In the reconstituted system, purified RPA coated with DNA, 9-1-1 complex, and Rad24-RFC are required for the stimulation of Mec1 activity toward Rad53 kinase dead or an artificial substrate PHAS-1. Omission of any of this component results in great compromise of Mec1 activation (Majka et al., 2006). Although the mechanism of how these multiple complexes contribute to the stimulation of Mec1 remains unclear, this in vitro results provide the initial evidence that activation of replication checkpoint is directly related with the recruitment of these complexes at stalled replication fork.

Chapter 2: Mechanism of Dun1 activation by Rad53 phosphorylation in *Saccharomyces cerevisiae*

2.1 Summary

Despite extensive studies, the molecular mechanism of DNA damage checkpoint activation remains incompletely understood. To better dissect this mechanism, we developed an activity-based assay for Dun1, a downstream DNA damage checkpoint kinase in yeast, using its physiological substrate Sml1. Using this assay, we confirmed the genetic basis of Dun1 activation. Rad53 was found to be directly responsible for Dun1 activation. We reconstituted the activation of Dun1 by Rad53 and found that phosphorylation of T380 in the activation loop of Dun1 by Rad53 is responsible for Dun1 activation. Interestingly, phosphorylation of the evolutionarily conserved T354 in the activation loop of Rad53 is also important for the regulation of Rad53 activity. Thus this conserved mode of activation loop phosphorylation appears to be a general mechanism for the activation of Chk2 family kinases.

2.2 Introduction

In S*accharomyces cerevisiae*, an evolutionarily conserved kinase cascade, consisting of Mec1, Tel1, Chk1, Rad53 and Dun1, is responsible for cellular responses to DNA damage (Nyberg et al., 2002). While Mec1 and Tel1 are involved in the initial detection of DNA damage (Jackson, 1996), Rad53 and Dun1 function as effector kinases to regulate many downstream cellular processes. Both Rad53 and Dun1 belong to the Chk2 family kinases, which contain Forkhead-associated (FHA) domain and serine/threonine kinase domain. DNA damage induced hyperphosphorylation of Rad53 and Dun1 in response to DNA damage depends on Mec1 (Sanchez et al., 1996). Further, adaptor proteins Rad9 and Mrc1 are important for DNA damage induced hyperphosphorylation of Rad53 (Alcasabas et al., 2001; Osborn and Elledge, 2003; Schwartz et al., 2002; Sun et al., 1998). Rad9 and Mrc1 become hyperphosphorylated in response to DNA damage treatment in a Mec1 and Tel1 dependent manner (Alcasabas et al., 2001; Emili, 1998; Tanaka and Russell, 2001; Vialard et al., 1998).

After DNA damage, Rad53 binds to hyperphosphorylated Rad9 and Mrc1 via its FHA domains. It was thus proposed that this interaction might be important for the activation of Rad53 *in vivo*. Rad53 activation appears to be accompanied by its autophosphorylation (Gilbert et al., 2001; Smolka, 2005). On the other hand, DNA damage induced phosphorylation of Dun1 was shown to depend on Rad53 and Rad53 could phosphorylate Dun1 *in vitro* (Bashkirov

et al., 2003; Lee et al., 2003). However, the activity of Dun1 was not measured directly. Since Dun1 acts genetically downstream of Mec1, Tel1, Rad9, Mrc1 and Rad53, understanding the regulation of Dun1 should further help to understand the activation of Rad53 and its upstream kinases Mec1 and Tel1. To this end, it is important to develop an activity-based assay for Dun1 and its upstream kinases using its physiological substrate.

Dun1 was originally identified as a mutant showing defect in the up-regulation of transcription of genes encoding ribonucleotide reductase (RNR) in response to DNA damage (Zhou and Elledge, 1993). It has been suggested that Dun1 involves in various DNA damage responses, including G2 arrest after DNA damage (Bashkirov et al., 2003; Gardner et al., 1999), in addition to the regulation of dNTP level after DNA damage. The RNR complex catalyzes the rate-limiting step in the synthesis of dNTP from NTP, which is crucial for DNA replication and repair. Multiple mechanisms were identified to regulate the dNTP level via the regulation of the RNR complex in the yeast *Saccharomyces cerevisiae*. First, transcription of the RNR genes is up-regulated in response to DNA damage, which is regulated by Dun1 (Huang et al., 1998). Second, Sml1, an inhibitor of RNR, is degraded in response to DNA damage (Zhao et al., 2001; Zhao et al., 1998). Importantly, Dun1 appears to be directly responsible for Sml1 phosphorylation and its subsequent degradation (Zhao and Rothstein, 2002). Finally, Dun1 dependent regulation of the localization of different RNR subunits in response to DNA damage

serves as additional mechanisms for the regulation of RNR activity in the cells (Lee and Elledge, 2006; Zhang et al., 2006). Taken together, it appears that an important function of Dun1 is the regulation of dNTP level in the cells. Several lines of evidence further suggested that Sml1 is a physiological substrate of Dun1. First, Sml1 was known to undergo Dun1-dependent degradation in response to DNA damage (Zhao and Rothstein, 2002). Second, Dun1 was shown to phosphorylate Sml1 efficiently *in vitro* (Zhao and Rothstein, 2002). Third, Dun1 interacts with Sml1 (Ho et al., 2002). Thus, phosphorylation of Sml1 by Dun1 may provide an assay to measure the kinase activity of Dun1.

In this study, we established an *in vitro* assay to quantify the activity of Dun1 for Sml1 hyperphosphorylation. Using this assay, we found that the activity of Dun1 is strongly induced after DNA damage treatment. Importantly, phosphorylation of Dun1 is required for this activity. Further, we confirmed and expanded the roles of Mec1, Tel1, Rad9 and Mrc1 in the activation of Dun1. Interestingly, deletion of *RAD53* completely abolished the activity of Dun1 for Sml1 hyperphosphorylation. We further reconstituted Dun1 activation using Rad53 and identified the phosphorylation sites of Dun1 using quantitative mass spectrometry (MS). Analysis of the phosphorylation-defective mutants of Dun1 revealed that T380 in the activation loop of the kinase domain of Dun1 is critical for Dun1 activation by Rad53 and DNA damage induced Sml1 degradation *in vivo*. Further, we identified that phosphorylation of the

conserved T354 in the activation loop of Rad53 regulates Rad53 activity. Our data thus suggested that phosphorylation of the conserved threonine residue in the activation loop of Dun1 and Rad53 is a key event to regulate their kinase activities.

.

2.3 Results

2.3.1 Activity of Dun1 is induced by DNA damage treatment and depends on its phosphorylation

To dissect the regulation of Dun1, we sought to develop an activity assay for Dun1, using its physiological substrate Sml1. To ask whether DNA damage treatment could activate Dun1, we compared the phosphorylation of Sml1 by Dun1-TAF that is epitope-tagged and integrated into the *DUN1* chromosomal locus, purified from either untreated or MMS-treated cells (we chose to analyze Dun1-TAF, since unpublished observations indicated that Dun1 over-expressed from either yeast or bacteria has a drastically reduced activity for Sml1 hyperphosphorylation). As shown in Figure 2.1A, MMS-treatment strongly enhanced the activity of Dun1 for Sml1 hyperphosphorylation. Importantly, prior treatment of the purified Dun1, using calf intestinal phosphatase (CIP), abolished the activity of Dun1 entirely. Therefore phosphorylation of Dun1 is essential for its ability to

hyperphosphorylate Sml1 (kinase-dead mutant of Dun1, purified using the same method, cannot hyperphosphorylate Sml1, see Fig. 2.4C later). An important feature of Sml1 hyperphosphorylation by Dun1 is a characteristic slower gel-shift of the hyperphosphorylated Sml1 compared to unphosphorylated Sml1 (see Fig. 2.1A, top panel). The ^{32}P incorporation of Sml1 is attributed to this hyperphosphorylated Sml1 (see Fig. 2.1A, middle panel).

To determine the efficiency of Sml1 hyperphosphorylation by Dun1, we examined the dependency of Sml1 hyperphosphorylation on varying concentrations of active Dun1 purified from MMS-treated cells. As shown in Figure 2.1B, increasing amounts of Dun1 led to more Sml1 hyperphosphorylation and its slower gel-shift. Quantification of hyperphosphorylated Sml1 revealed that there is an approximately linear relationship between the amount of hyperphosphorylated Sml1 and the concentration of Dun1 when the Dun1 concentration is less than 1.6 nM (see Fig. 2.1C). This is expected since unphosphorylated Sml1 is in great excess compared to Dun1. At higher Dun1 concentrations, phosphorylation of Sml1 appeared to reach saturation and most of Sml1 was converted into a hyperphosphorylated form (see Fig. 2.1B). Therefore, for accurate comparison of Dun1 activity, the amount of Dun1 used here is always in the linear range where approximately half of Sml1 remains unphosphorylated.

2.3.2 Genetic analysis of Dun1 activation reveals the roles of various DNA damage checkpoint genes

Mec1 and Tel1 are known to function at the top of the kinase cascade in the DNA damage checkpoint. We therefore asked how Dun1 activity might depend on Mec1 and Tel1. As shown in Figure 2.2A, deletion of *MEC1* greatly diminished the activity of Dun1 in either un-treated or MMS-treated cells, compared to WT cells. On the other hand, deletion of *TEL1* diminished the activity of Dun1 in the absence of MMS treatment. After MMS treatment, Dun1 was activated in *tel1Δ* cells, similar to that in WT cells. Interestingly, deletion of both *MEC1* and *TEL1* completely abolished the activity of Dun1 (also see Fig. 2.2D). The ^{32}P incorporation in the phosphorylated Sml1, excised from the gel, was quantified using scintillation counting, which confirmed the relative contributions of Mec1 and Tel1 in Dun1 activation.

Rad9 and Mrc1 are adaptor proteins in the DNA damage and replication checkpoints. We next asked whether they could play a role in Dun1 activation using the same Sml1 phosphorylation assay. As shown in Figure 2.2B, deletion of *RAD9* reduced the activity of Dun1 in both untreated and MMS treated cells, compared to that in WT cells. Interestingly, deletion of *MRC1* alone led to a much higher activity of Dun1 than that of Dun1 in WT cells in the absence of MMS treatment. MMS treatment of the *mrc1Δ* cells resulted in a higher activity of Dun1, which is similar to that of WT cells after MMS treatment. Further, deletion of both *RAD9* and *MRC1* greatly diminished

the activity of Dun1, although a residual activity of Dun1 in *rad9Δ mrc1Δ* cells does exist (Figure 2.2D). Therefore Rad9 and Mrc1 act redundantly for Dun1 activation *in vivo*. While Rad9 appears to only promote Dun1 activation in response to DNA damage, Mrc1 has a dual role. First, Mrc1 prevents Dun1 activation in the absence of exogenous DNA damage treatment. Second, Mrc1 acts redundantly with Rad9 to facilitate DNA damage induced Dun1 activation. Together, Rad9 and Mrc1 are critical for the activation of Dun1.

Rad53 and Chk1 are thought to be effector kinases in the DNA damage checkpoint. Rad53, in particular, was shown to interact with Dun1 and be able to phosphorylate Dun1 *in vitro* (Bashkirov et al., 2003; Lee et al., 2003). We thus examined the roles of Rad53 and Chk1 in the activation of Dun1. The activities of Dun1 in *rad53Δ*, *chk1Δ* and *rad53Δ chk1Δ* mutants were quantified. Deletion of *RAD53* completely abolished the activity of Dun1 in both untreated and MMS-treated cells, while deletion of *CHK1* alone had no detectable effect (see Fig. 2.2C). Therefore, Rad53 is required for Dun1 activation *in vivo*. To better examine the residual activity of Dun1 in *rad53Δ*, *mec1Δ*, *mec1Δ tel1Δ* and *rad9Δ mrc1Δ* cells, 5-fold more Dun1 (10 ng), compared to the amount used in Figs. 2.2A~2C, was used to phosphorylate Sml1. As shown in Figure 2.2D, Dun1 purified from *rad53Δ* cells is completely defective in Sml1 hyperphosphorylation, although a *hypo*-phosphorylated Sml1 was detected. Similarly Dun1 purified from *mec1Δ tel1Δ* cells is completely defective in Sml1 hyperphosphorylation. Interestingly, Dun1 has a

weak, however readily detectable activity for Sml1 hyperphosphorylation in *mec1Δ* cells, which is induced by MMS treatment. This activity is presumably dependent on Tel1 because deletion of both *MEC1* and *TEL1* abolished the activity of Dun1 completely (see Fig. 2.2D). Finally Dun1 in *rad9Δ mrc1Δ* cells could still hyperphosphorylate Sml1. This observation suggested that Mec1 and Tel1 could bypass the requirement of Rad9 and Mrc1 to activate Rad53 and Dun1; however, this activation is far less than that in WT cells.

2.3.3 In vitro activation of Dun1 by Rad53 for Sml1 hyperphosphorylation

Since Rad53 is required for Dun1 activation *in vivo*, we next asked whether recombinant Rad53 could activate Dun1 for Sml1 hyperphosphorylation *in vitro* (recombinant Rad53 alone does not hyperphosphorylate Sml1, unpublished observation). As shown in Figure 2.3A, WT Rad53 shows a reduced electrophoretic mobility compared to Rad53-KD, which is due to its autophosphorylation. Rad53-4TA has a similar electrophoretic mobility as WT Rad53. As shown in Figure 2.3B, recombinant WT Rad53 activated WT Dun1, purified from *rad53Δ* cells, for Sml1 hyperphosphorylation, while Dun1-D328A or Dun1-KD, failed to be activated by WT Rad53 (Fig. 2.3B). Thus, the kinase activity of Dun1 is required for Sm1 hyperphosphorylation. Next we asked whether a known interaction between the N-terminal 4TQ phosphorylation cluster of Rad53 and FHA domain of Dun1 is important for Rad53 to activate Dun1 (Lee et al., 2003). As shown in Figure 2.3B, the same amount of recombinant Rad53-4TA mutant kinase

failed to activate WT Dun1 for Sml1 hyperphosphorylation. Conversely, Dun1-R60A, N103A, in which the binding capacity of Dun1 FHA domain is compromised by the R60A and N103A mutations, failed to be activated by WT Rad53 as expected. Therefore the interaction between the N-terminal 4TQ phosphorylation cluster of Rad53 and Dun1 FHA domain is important for the activation of Dun1 by Rad53.

Since phosphorylation of Dun1 is essential for its activity, we identified the phosphorylation sites of endogenous Dun1 in WT cells after MMS treatment using MS (Smolka, 2005). More than twenty phosphorylation sites were detected in four regions of Dun1, including the N-terminal region, the region between the FHA and kinase domains, the activation loop of the kinase domain, and C-terminal region (see Fig. 2.3C). Next, we identified the phosphorylation sites of Dun1 (purified from *rad53Δ* cells) before and after Rad53 phosphorylation *in vitro*. Few phosphorylation of Dun1 was detected in *rad53Δ* cells. After *in vitro* phosphorylation by Rad53, the phosphorylation sites of Dun1 were again identified. Interestingly, the DNA damage induced phosphorylation sites of endogenous Dun1 and the *in vitro* phosphorylation sites of Dun1 by Rad53 are essentially the same. Therefore Rad53 is directly responsible for Dun1 phosphorylation.

To identify possible autophosphorylation sites of Dun1, we used the N-isotag technology to quantitatively compare the relative abundance between WT Dun1 and Dun1-KD, i.e. Dun1-D328A, after MMS treatment (Smolka,

2005). As shown in Fig. 3D, the abundance of two phosphopeptides containing S10 and S139, respectively, is greatly reduced in Dun1-KD, compared to WT Dun1, while the abundance of other Dun1 phosphopeptides are essentially unchanged between WT Dun1 and Dun1-KD. Therefore S10 and S139 are autophosphorylation sites of Dun1 (see Fig. 2.3D). Next we used quantitative MS to quantify the abundance changes in phosphorylation of Dun1-KD (purified from unperturbed cells), following its *in vitro* phosphorylation by Rad53. The S/T residues of Dun1 that were strongly phosphorylated by Rad53 were determined (see Fig. 2.3D), while the others were much less phosphorylated and thus not shown. Interestingly, these highly phosphorylated sites of Dun1 by Rad53 all have a bulky and hydrophobic residue at the +1 position relative to the phosphorylated Ser/Thr residue (see Fig. 2.3D).

2.3.4 Phosphorylation of T380 of Dun1 is critical for its kinase activity

As shown above, several phosphorylation sites of Dun1 were found, including autophosphorylation sites S10 and S139, and a number of trans-phosphorylation sites including T380, S195 and others. To ask whether these phosphorylation sites of Dun1 might be important for its function, we next examined the sensitivities of various Dun1 phosphorylation-defective mutants, including *dun1-S10A*, *dun1-S139A*, *dun1-S195A* and *dun1-T380A*, to DNA replication stress caused by hydroxyurea or UV treatment. First we confirmed that various Dun1 phosphorylation-site mutants have similar abundance in

cells (see Fig. 2.4A). As shown in Figure 4B, mutations to S10 and S139 of Dun1 rendered the cells more sensitive to HU and UV treatments. Therefore, autophosphorylation of Dun1 is functionally important. On the other hand, S195A mutation has little effect. Unpublished observations indicated that mutations to other SF/TF sites of Dun1 did not inactivate Dun1 and thus not investigated further. Interestingly, *dun1-T380A* is very sensitive to both HU and UV treatments. We then examined the activity of Dun1-T380A and compared it to those of WT Dun1 and a kinase-inactive allele of Dun1, i.e., Dun1-KD or Dun1-D328A. As shown in Figure 4C, while WT Dun1 showed MMS-induced activation, Dun1-KD is completely inactive as expected. Interestingly, Dun1-T380A is also completely defective in Sml1 hyperphosphorylation. Dun1-T380A did phosphorylate Sml1 into a hypo-phosphorylated form, which is not slower-shifted in the gel compared to the hyperphosphorylated Sml1 by WT Dun1. Therefore phosphorylation of T380 of Dun1 enables Dun1 to hyperphosphorylate Sml1.

2.3.5 Dun1 activity is inversely correlated with Sml1 abundance in cells and it is regulated by T380 phosphorylation

Since Dun1 is important for DNA damage induced degradation of Sml1 *in vivo*, we asked whether the activity of Dun1 for Sml1 hyperphosphorylation is correlated with the abundance of Sml1 in cells. As shown in Figures 2.5A, Sml1 abundance is reduced in *mrc1D* cells compared to that in WT. In contrast, Sml1 appears to be more abundant in *rad9D* cells in the absence of

MMS treatment. After MMS treatment, the abundance of Sml1 is reduced in both cases. We next examined the abundance of GFP-Sml1 in *dun1-T380A* cells because *dun1-T380A* is hypersensitive to genotoxic stresses and Dun1-T380A fails to hyperphosphorylate Sml1 (see Fig. 2.4C). T380A mutation of Dun1 led to a greatly elevated Sml1 abundance in cells with or without MMS treatment, which is similar to that in *dun1D* and *dun1-KD* cells (see Fig. 2.5B). To quantitatively compare the abundance of Sml1 in various mutants, anti-GFP Western blot was used. In the absence of MMS treatment, the abundance of Sml1 is reduced in *mrc1D* cells, compared to that in WT or *rad9D* cell (see Fig. 2.5C). Further, Sml1 abundance in *rad9D* cells is higher than that in WT cells in the absence of MMS treatment. With the assumption that the abundance of Sml1 should be inversely correlated with Dun1 activity, these observations are consistent with the activities of Dun1 found in *rad9D* and *mrc1D* cells (see Fig. 2.2B). Importantly, Sml1 abundance in *dun1(T380A)* cells is the same as that in *dun1-KD* and *dun1D* mutants and it failed to be degraded after MMS treatment. Therefore the ability of Dun1 to hyperphosphorylate Sml1 is inversely correlated with the abundance of Sml1 and it is required for MMS-induced Sml1 degradation in cells.

2.3.6 Phosphorylation of T354 of Rad53 is important for Rad53 activity and functions *in vivo*

Since T380 of Dun1 locates in the activation loop of the Dun1 kinase domain and activation loop phosphorylation was often found to be important

for activities of many kinases (Johnson et al., 1996), we performed a sequence alignment of the activation loops of various Dun1 homologs and found that T380 of Dun1 is strictly conserved in the Chk2 family kinases, including T354 of Rad53 (see Fig. 2.6A). Interestingly, T354 of Rad53 is followed by a hydrophobic phenylalanine at its +1 position. Phosphorylation of T354 of Rad53 was found previously (Sweeney et al., 2005). We re-examined our previous data on the phosphorylation of Rad53 and found that phosphorylation of T354 is induced by MMS treatment and it is an autophosphorylation site of Rad53 (Smolka, 2005). To ask whether phosphorylation of T354 of Rad53 regulates its kinase activity, we generated a *rad53-T354A* mutant. As shown in Figure 6B, similar to Rad53-KD, Rad53-T354A has a reduced MMS induced hyperphosphorylation and slower electrophoretic gel-shift, compared to WT Rad53. We next examined the activity of Rad53 to activate Dun1 for Sml1 hyperphosphorylation. As shown in Figure 6B, hyperphosphorylation of Sml1 was greatly reduced when Rad53-T354A was used, compared to WT Rad53. Quantification of the ^{32}P labeled Sml1 using scintillation counting indicated a 20-fold reduction of the amount of hyperphosphorylated Sml1 when Rad53-T354A was used (see Fig. 2.6B, right panel). Although much reduced, Rad53-T354A does have a residual activity to activate Dun1 for Sml1 hyperphosphorylation. As expected, Rad53-KD failed to activate Dun1 for Sml1 hyperphosphorylation completely.

We next examined the sensitivity of *rad53-T354A* cells to various

genotoxic stresses. First, *rad53-T354A* cells have a similar growth rate as WT cells, while *rad53-KD* and *rad53D* cells grow slower. This might be related to the fact that Rad53-T354A is not completely inactive. Second, compared to WT cells, *rad53-T354A* cells are hypersensitive to UV and HU treatments (see Fig. 2.6C). Taken together, phosphorylation of T354 of Rad53 is important for Rad53 activity and functions *in vivo*. Because phosphorylation of T354 was found in recombinant Rad53 and it is followed by a phenylalanine, phosphorylation of T354 of Rad53 appears to be a result of its autophosphorylation.

2.4 Discussion

2.4.1 The Dun1-Sml1 assay is a sensitive and reliable assay to dissect the pathway of Dun1 activation

Dun1 was known to function downstream in the kinase cascade in the DNA damage checkpoint, which has been extensively studied previously (Bashkirov et al., 2003; Lee et al., 2003; Nyberg et al., 2002; Sanchez et al., 1996; Sun et al., 1996; Sun et al., 1998). Here, we sought to establish an *in vitro* activity assay to monitor Dun1 activity, using its physiological substrate Sml1. This assay, once established, will be used to reconstitute the activation of Dun1 and its upstream kinases. To validate the Dun1-Sml1 assay, we used it to examine the roles of various known DNA damage checkpoint proteins in Dun1 activation. Our observations are summarized in Figure 2.7A, which

essentially recapitulate existing knowledge of this pathway. As expected, Mec1 is primarily responsible for DNA damage induced Dun1 activation, while Tel1 plays a much less important role. Interestingly, the observation that Dun1 activity is completely abolished in *mec1D tel1D* cells, but not *mec1D* cells (see Fig. 2.2D), indicated that Tel1 does play a role in controlling Dun1 activity.

Rad9 and Mrc1 are adaptor proteins that were known to interact with Rad53 (Alcasabas et al., 2001; Schwartz et al., 2002; Sun et al., 1998; Tanaka and Russell, 2001; Xu et al., 2006). As expected, Rad9 is important for Dun1 activation. Interestingly, a novel dual function of Mrc1 in Dun1 activation was identified, including a role in promoting MMS-induced Dun1 activation and preventing Dun1 activation in the absence of exogenous DNA damage treatment. Mrc1 was known to function in the maintenance of DNA replication fork (Alcasabas et al., 2001; Osborn and Elledge, 2003; Tanaka and Russell, 2001). Recently, it was shown that deletion of *MRC1* causes slowing of DNA replication fork progression, possibly defects in replication fork maintenance and thus damaged DNA in the cells (Szyjka et al., 2005). Up-regulation of RNR gene transcription was also observed in *mrc1D* cells (Pan et al., 2006). These observations are consistent with our observations that Dun1 is activated in unperturbed *mrc1D* cells (see Fig. 2.2B) and Sml1 abundance is diminished in *mrc1D* cells (see Fig. 2.5A). On the other hand, Mrc1 is also important for the activation of Dun1 in response to DNA damage (see Figs. 2.2B and 2.2D).

In agreement with previous studies (Bashkirov et al., 2003; Lee et al., 2003), we found that Rad53 is directly responsible for Dun1 activation. Since Rad53 was known to function downstream of Mec1, Tel1, Rad9 and Mrc1, our results thus recapitulated the known genetic pathway of Dun1 activation (see Fig. 2.7A). Taken together, these observations indicated that the Dun1-Sml1 assay is a sensitive and reliable assay to study DNA damage checkpoint activation in yeast.

2.4.2 Consensus phosphorylation site of Rad53 and autophosphorylation site of Dun1

Quantitative analysis of the phosphorylation sites of Dun1 using quantitative MS revealed new insights into the preferred phosphorylation sites of Rad53 and Dun1. Using quantitative MS, several strongly phosphorylated sites of Dun1 by Rad53 were determined. Interestingly all of them appear to have a bulky hydrophobic residue at the +1 position relative to the phosphorylated Ser/Thr residues, including T380 of Dun1 (see Fig. 2.3D). Phosphorylation of both the T380 of Dun1 and T354 of Rad53 are critical for their respective activities. Importantly, both are followed by a hydrophobic residue at the +1 position. Thus Rad53 appears to prefer to phosphorylate Ser/Thr followed by a bulky hydrophobic residue. We further identified the autophosphorylation sites of Dun1 and they include S10 and S139 (see Fig. 2.3D). Interestingly, the SSSST sequence of Dun1 (residue 139-143) was found to be hyperphosphorylated. It was known that Dun1

hyperphosphorylates a serine cluster in Sml1 (Uchiki et al., 2004). Therefore Dun1 may prefer to phosphorylate Ser/Thr clusters. Characterization of additional Dun1 substrates should further help to establish the consensus phosphorylation motif for Dun1. In summary, the preferred phosphorylation sites of Rad53 and Dun1 identified here should facilitate functional studies of additional Rad53 and Dun1 substrates in the future.

2.4.3 Phosphorylation regulation of Dun1 and Rad53

Hyperphosphorylation of Rad53 and Dun1 were known to occur in response to DNA damage treatment (Sanchez et al., 1996; Sun et al., 1996; Zhou and Elledge, 1993). However, the key phosphorylation site that regulates their activities was not determined. We have established an *in vitro* assay to activate Dun1 by recombinant Rad53 (see Fig. 2.3B). Using this assay, we showed that the interaction between the N-terminal TQ phosphorylation cluster of Rad53 and the FHA domain of Dun1 promotes Dun1 activation by Rad53. Mutation to either the FHA domain of Dun1 or the 4TQ cluster in the N-terminal region of Rad53 diminished the ability of Rad53 to activate Dun1 for Sml1 hyperphosphorylation (see Fig. 2.3B).

Rad53 phosphorylates Dun1 on many serine and threonine residues (see Fig. 2.3C). Because phosphorylation of T380 of Dun1-KD purified from MMS treated cells is similar to that of WT Dun1 and T380 is strongly phosphorylated by Rad53 *in vitro* (see Fig. 2.3D), Rad53 appears to be directly responsible for phosphorylation of T380 of Dun1. Importantly, this residue resides in the

activation loop of Dun1 kinase domain and it is conserved in various Chk2 family kinases, including Rad53. Despite numerous autophosphorylation sites of Rad53 exist, phosphorylation of a single conserved T354 of Rad53 was found to play a crucial role in controlling Rad53 activity. Importantly, T354 of Rad53 agrees with our proposed consensus phosphorylation site of Rad53 and it is an autophosphorylation site. In summary, a model of Dun1 activation by Rad53 is proposed (see Fig. 2.7B) (Bashkirov et al., 2003; Lee et al., 2003). We suggest that autophosphorylation of T354 activates Rad53, which then phosphorylates the T380 of Dun1 to activate Dun1.

Further study is needed to elucidate the molecular mechanism of Rad53 activation. Rad9 and Mrc1 likely play a direct role, although direct Mec1 phosphorylation of Rad53 may also contribute to its activation (Ma et al., 2006; Sweeney et al., 2005; Xu et al., 2006). This Dun1-Sml1 assay could be used to examine these possibilities and reconstitute the activation of the kinase cascade in the DNA damage checkpoint. It is interesting to also note that phosphorylation of the conserved T383 in the activation loop of human Chk2 was also found to be important for Chk2 activity (Lee and Chung, 2001). While phosphorylation of the N-terminal TQ site of Chk2 family kinases is widely believed to be important for their activities, our result strongly suggest that phosphorylation of this conserved threonine residue in the activation loop appears to be a conserved and key mechanism of the activation of Chk2 family kinases.

2.5 Methods

2.5.1 Yeast strains, plasmids and genetic methods

Standard yeast growth and genetic methods are used in this work. Strains used in this work are listed in Supplementary Table S1. Plasmids used in this work are listed in Supplementary Table S2. GFP-Sml1 was first cloned into pFA6a plasmid using PacI and AscI, then introduced into yeast cells via homologous recombination (Longtine et al., 1998). C-terminal TAF tagged Dun1 was cloned into a pFA6a plasmid, yielding pFA6a-Dun1TAF-KanMX6 plasmid. Site-directed mutagenesis was used to generate various Dun1 mutants in this plasmid, which were then used to generate endogenous Dun1 mutants using homologous recombination. The TAF tag contains a 6xHis-3xFLAG-Protein A, with a TEV protease cleavage sequence between the 3xFLAG sequence and Protein A. This allows the elution of Dun1 using TEV protease. After TEV cleavage, a remaining 3XFLAG sequence at the C-terminus of Dun1 allows the detection of Dun1 using anti-FLAG Western blot. Deletion of Sml1 suppresses the lethality of *MEC1* and *RAD53* deletion, as well as synthetic lethality of *RAD9* and *MRC1* deletion. For Dun1 activity study, *sml1Δ* background was therefore used unless noted otherwise (unpublished observation indicated that deletion of *SML1* does not affect Dun1 activity in WT cells). All mutations or integrations introduced in yeast cells were confirmed by DNA sequencing.

Sml1 was cloned into pGEX-4T1 using BamHI and EcoRI sites.

Recombinant Rad53 was cloned into a pET21a plasmid with an N-terminal Protein A tag using EcoRI and NotI sites. Site-directed mutagenesis was used to generate Rad53-T354A mutant. To generate Rad53-4TA, which contains a quadruple mutation including T5A, T8A, T12A and T15A, a primer containing these mutations was used to PCR-amplified Rad53 sequence and subcloned into pET21a plasmid. WT and mutant Rad53 were cloned into a pFA6a plasmid with or without a C-terminal TAF tag, which were then used to transform into yeast cells to generate endogenous Rad53 mutants. DNA sequencing was performed to verify the sequence in each case.

2.5.2 Protein purification techniques and CIP treatment

For purification of Dun1, 50 ml of yeast culture was used. Cells were either untreated or treated by 0.05% MMS for 2 hours, then harvested. Dun1-TAF in various yeast mutants was affinity-purified using IgG resin and eluted after TEV protease cleavage. For calf intestinal phosphatase (CIP) treatment, Dun1-TAF bound to the IgG resin was incubated with 10 units of CIP (New England Lab) in 50 ml of NEB buffer 3 at 37 °C for 1 hour, washed by TBS, then eluted after cleavage using 10 units of TEV protease at 30°C for 1 hour. The amount of Dun1 was quantified and normalized using quantitative anti-FLAG Western blot and Silver staining. To purify recombinant Rad53, N-terminal Protein A tagged Rad53 was affinity purified using IgG resin and eluted after TEV protease cleavage. To purify recombinant GST-Sml1, glutathione-affinity chromatography was used according to manufactory's

recommendation.

2.5.3 *In vitro* kinase assay

In a typical kinase assay, 50 mM Tris, pH7.5, 150mM NaCl, 0.1% Tween 20, 0.2 mM ATP, 10mM $MgCl_2$, 10 μCi of ^{32}P-ATP were used. 2ng of Dun1 and 2 μg of GST-Sml1 was always used unless indicated otherwise. The amount of Rad53 or Dun1 used is indicated in the figure legend. One-hour kinase reaction at 30 °C was always used.

2.5.4 Dun1 phosphorylation analysis using quantitative mass spectrometry

To identify MMS induced phosphorylation of endogenous Dun1, approximately 8 grams of Dun1-TAF cell pellet were used to purify approximately 2 μg of Dun1. Similar amounts of Dun1 purified from *rad53Δ* cells were used for MS analysis of the phosphorylation of Dun1 with or without *in vitro* Rad53 phosphorylation. For quantitative comparison of Dun1 phosphorylation, the same amount of Dun1 to be compared was digested by trypsin, labeled by an N-isotag reagent as described previously (Smolka, 2005). Here we used D0 (no deuterium) or D10 (10 deuterium) containing Boc-Leu-NHS ester, instead of Boc-GABA-NHS esters used previously (Smolka, 2005). With or without N-isotag labeling, phosphopeptides of Dun1 were purified using immobilized metal affinity column and analyzed as described previously (Smolka, 2005). Database search was performed with no

restriction on the enzyme used for proteolysis and the entire yeast database was used. Only doubly tryptic phosphopeptides were considered and manually verified.

2.6 Acknowledgments

We thank excellent technical assistance from Xiao Wei. Dr. Rodney Rothstein for a generous gift of the YFP-Sml1 strain during our initial study and stimulating discussion. Dr. Richard Kolodner and Dr. Christopher Putnam for critical reading of the manuscript. This work is supported by a K22 Faculty transition grant from NHGRI (HG002604) and additional research support from the Ludwig Institute for Cancer Research to H.Z.

This chapter has appeared in print under the following citation: Chen, S.-H., Smolka, M.B., and Zhou, H. (2007) Mechanism of Dun1 activation by Rad53 phosphorylation in Saccharomyces cerevisiae. Journal of Biological Chemistry 282, 986-995. The dissertation author was the primary author of this paper.

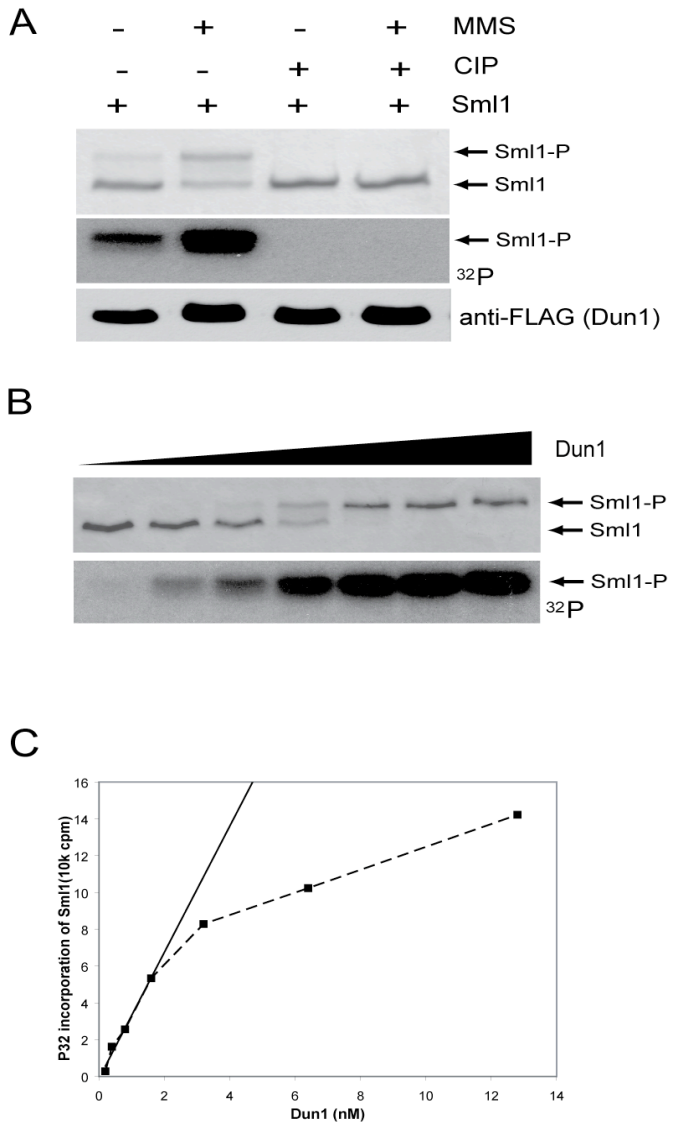

Figure 2.1 Analysis of Dun1 activity using Sml1

A) Endogenous Dun1 purified from untreated or MMS treated Dun1-TAF cells was assayed for its kinase activity. Top panel: Coomassie staining of Sml1 after each kinase reaction. Middle panel: autoradiography of Sml1. Bottom panel: anti-FLAG Western blot shows the loading control of Dun1. B) Dependence of Sml1 hyperphosphorylation on the concentrations of Dun1 purified from MMS-treated Dun1-TAF cells. A 2-fold increase of Dun1, starting from 0.2 nM, was used to phosphorylate Sml1 (2.5 mM). Upper panel: Coomassie staining of Sml1. Lower panel: autoradiography of Sml1. C) The amount of phosphorylated Sml1 was quantified using scintillation counting. An approximate linear relationship was found between the concentration of Dun1 and the amount of Sml1 phosphorylation when Dun1 concentration is low.

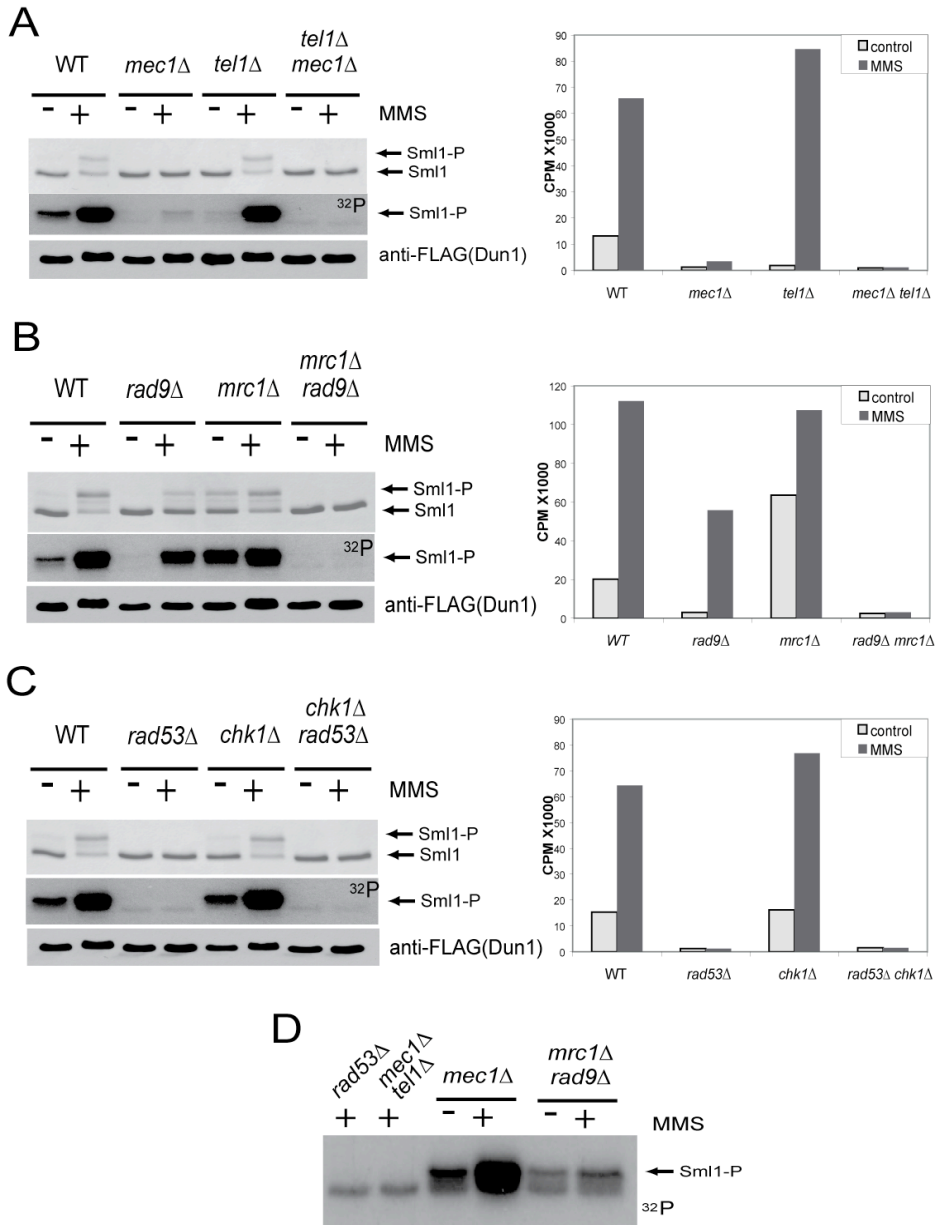

Figure 2.2 Analysis of Dun1 activity purified from various mutant backgrounds

Upper panel: Coomassie staining of Sml1. Middle panel: autoradiography of Sml1. Bottom panel: anti-FLAG Western blot shows the loading control of Dun1 used. A) Effect of MEC1 and TEL1 deletion on Dun1 activity. B) Effect of RAD9 and MRC1 deletion on Dun1 activity. C) Effect of RAD53 and CHK1 deletion on Dun1 activity. D) Closer examination of Dun1 activity in various checkpoint mutants, using five fold more (10 ng) of Dun1 purified from each mutant.

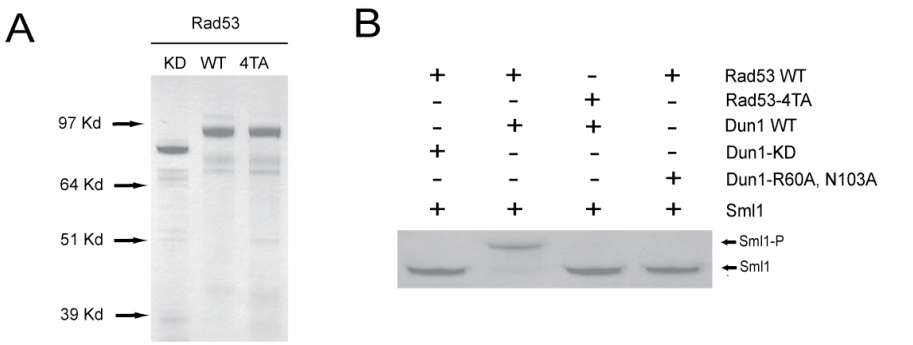

C

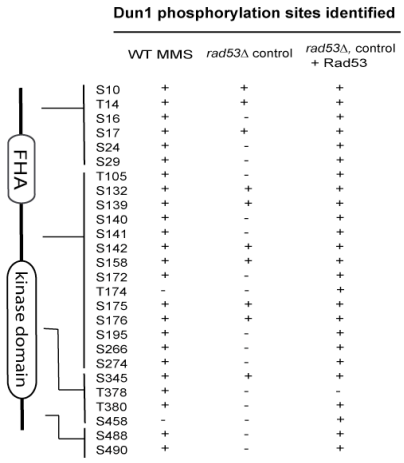

D

Fold change of Dun1 phosphorylation		
Site	Dun1 KD (+/- Rad53) in vitro	MMS Dun1 (WT/KD) in vivo
S10	2	11
S17	10	1
T105	30	N/D
S132	6	4
S139	1	23
S158	11	2
S195	>100#	1
S266	>100#	2
T380	9	1

Rad53 trans-phosphorylation site

```
      ++
12    DVTDSSFKRQQ
100   KSRNGTFINGN
127   FGKSCSFLFKY
153   SSESRSYKNDD
190   KTRPVSFFDKY
261   VNLLDSFVEPI
375   MQFTNTLCGTP
```

(S/T)(F/Y/L)

Dun1 auto-phosphorylation site

```
      +
5     TKREHSGDVTD
134   LFKYASSSSTD
```

Figure 2.3 *In Vitro* Reconstitution of Dun1 phosphorylation State

A) Commassie staining of purified recombinant Rad53 including wild type, 4TA mutant, and kinase-dead mutant. B) In vitro activation of Dun1 using Rad53. 1ng of WT or 4TA mutant Rad53 was used. C) Phosphorylation maps of Dun1 revealed that Rad53 is entirely responsible for Dun1 phosphorylation. D) Summary of autophosphorylation sites of Dun1 and the Rad53 induced transphosphorylation sites of Dun1 identified using quantitative MS. N/D: not determined. #: indicates that the corresponding phosphopeptide without Rad53 phosphorylation was not detected, thus the value refers to signal to noise ratio. +: indicates the phosphorylated Ser/Thr. *: indicates the residue at the +1 position.

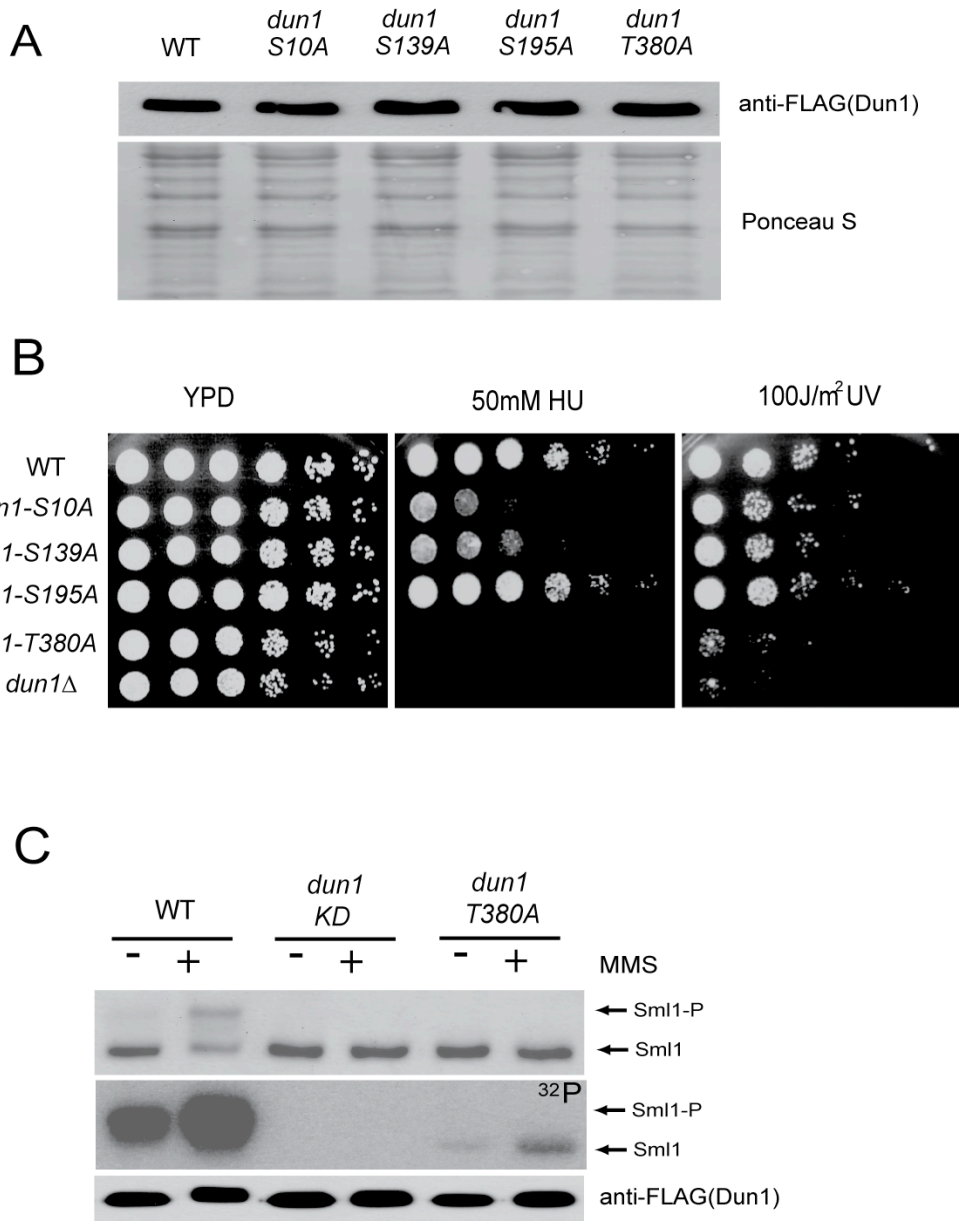

Figure 2.4 Phenotypes of Dun1 phosphorylation sites mutants
A) Western blot analysis of the abundance of WT Dun1 and various Dun1 phosphorylation-site mutants with the control of Ponceau S staining of the same. B) UV and hydroxyurea sensitivities of various Dun1 phosphorylation-defective mutants. A serial dilution of various cells was spotted on either HU-containing YPD plate or YPD plate and subjected to UV treatment. C) Comparison of the activity of WT, Dun1-KD and Dun1-T380A for Sml1 hyperphosphorylation

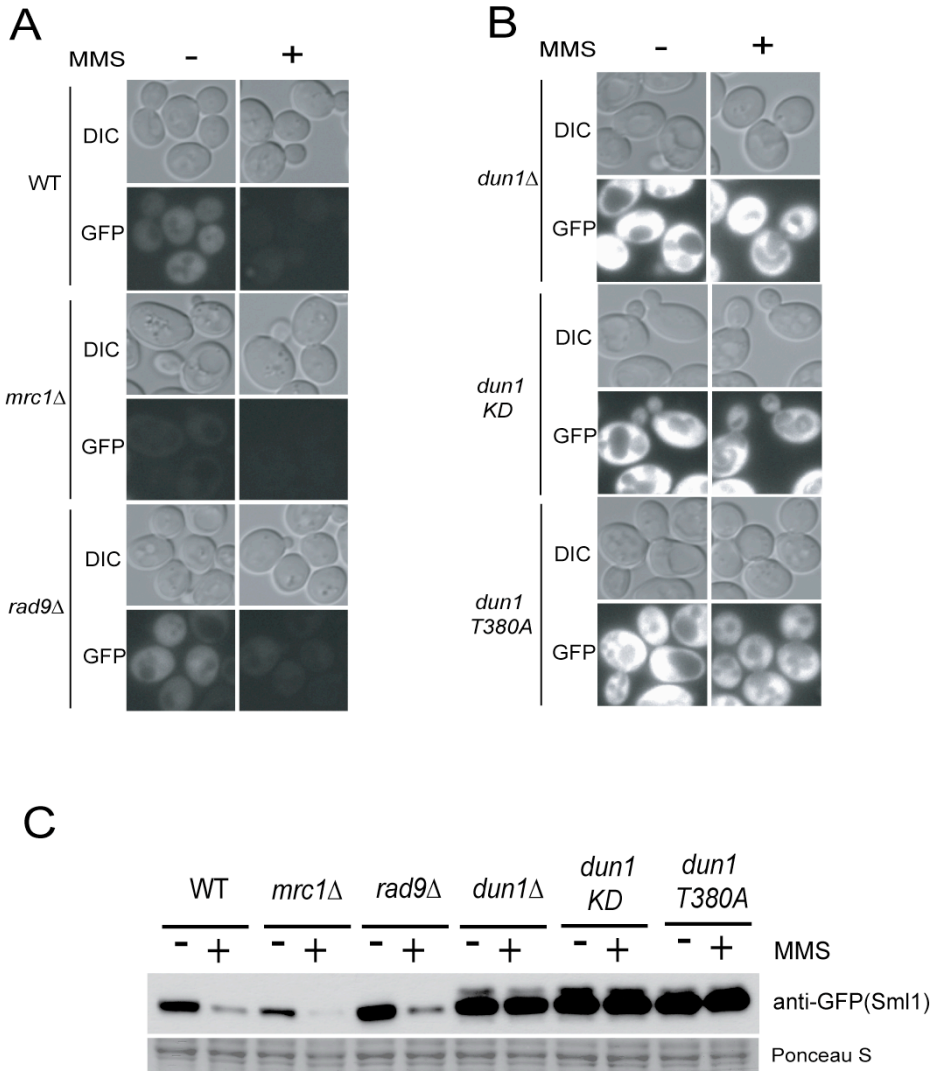

Figure 2.5 GFP-Sml1 abundance in rad9Δ , mrc1Δ and dun1-T380A mutants

A) Sml1 abundance is analyzed in *rad9Δ* and *mrc1Δ* cells. B) GFP-Sml1 abundance in dun1-T380A cells is similar to *dun1-KD* in response to MMS treatment. C) Anti-GFP western blot analysis of GFP-Sml1.

A

```
                                                +*
Dun1 Saccharomyces cerevisiae  365 DFGLAKFTG-EMQFTNTLCGTPSYVAPE
Rad53 Saccharomyces cerevisiae 339 DFGLAKVQG-NGSFMKTFCGTLAYVAPE
Cds1 Schizosaccharomyces pombe 312 DFGLAKVIHGTGTFLETFCGTMGYLAPE
Loki Drosophila melanogaster   307 DFGLSKFVQ-KDSVMRTLCGTPLYVAPE
Cds1 Xenopus laevis            340 DFGQSKILG-ETSLMRTLCGTPTYLAPE
Chk2 Mus musculus              372 DFGQSKILG-ETSLMRTLCGTPTYLAPE
Chk2 Homo sapiens              368 DFGHSKILG-ETSLMRTLCGTPTYLAPE
```

B

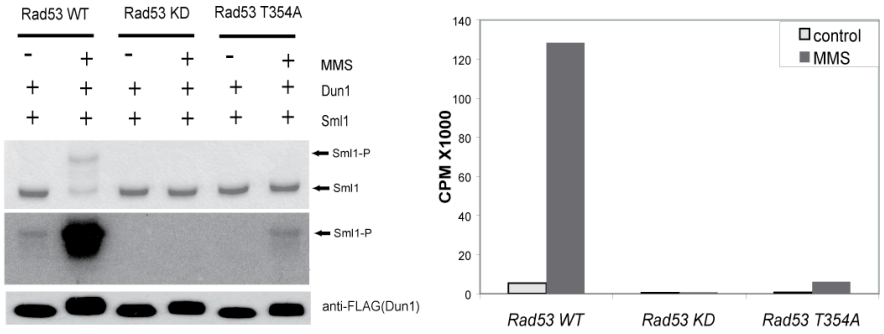

C

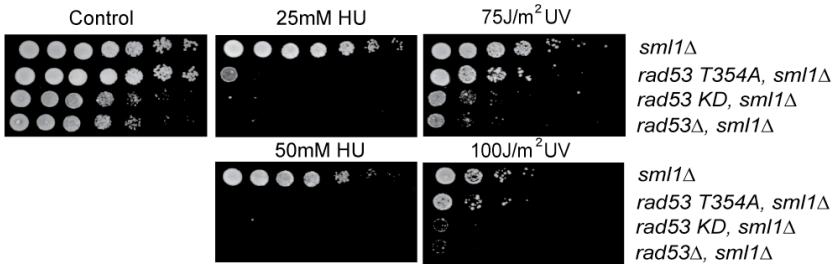

Figure 2.6 Rad53 activation loop phosphorylation is involved in its activation

A) Sequence alignments of various Dun1 orthologs, indicating that T380 in the activation loop of Dun1 kinase domain is conserved in the Chk2 family kinases. +: indicates the conserved Thr residue. *: indicates the residue at the +1 position. B) Sml1 hyperphosphorylation assay using 50 pg of Rad53 and 2ng of Dun1 purified from rad53Δ cells. Upper panel: Coomassie staining of Sml1. Middle panel: 32P labeling of Sml1. Lower panel: anti-FLAG WB detects Dun1. Right panel: scintillation counting of the amount of 32P incorporation of the phosphorylated Sml1. C) UV and hydroxyurea sensitivities of WT, *rad53-KD*, and *rad53-T354A* mutant.

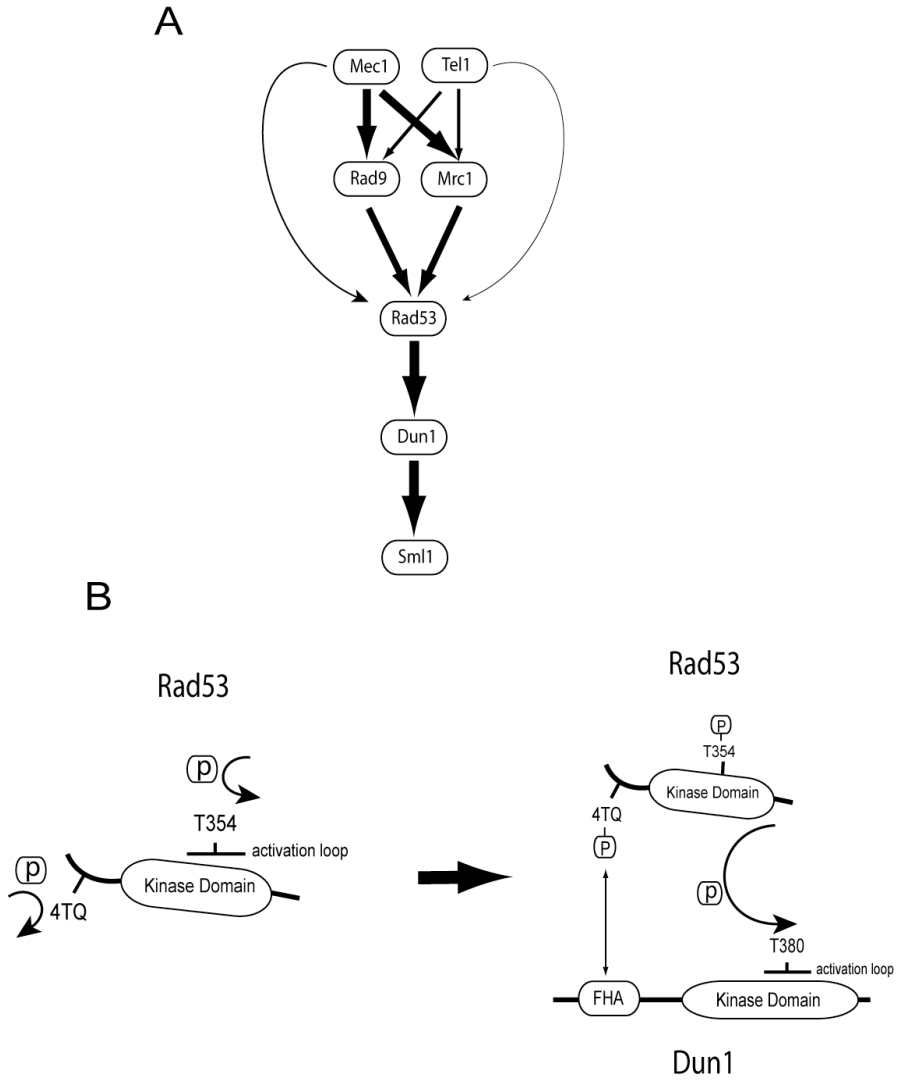

Figure 2.7 Model for Dun1 and Rad53 activation

A) Summary of the roles of various upstream proteins in Dun1 activation. A thicker arrow indicates a larger contribution to Dun1 activation. B) A model on Dun1 activation via Rad53 phosphorylation. Rad53 is autophosphorylated on T354, which activates Rad53. Phosphorylated Rad53 also interacts with Dun1 via the FHA domain of Dun1 and the N-terminal phosphorylation cluster of Rad53. This interaction facilitates the phosphorylation of T380 of Dun1 by Rad53, leading to Dun1 activation.

Table 2.1 Yeast strains used in this study

Strain	Genotype	Reference / Source
RDKY3023	*MATa, ura3-52, leu2Δ1, trp1Δ63, his3Δ200, lys2ΔBgl, hom3-10, ade2Δ1, ade8*	Richard Kolodner
RDKY2669	*MATα, ura3-52, leu2Δ1, trp1Δ63, his3Δ200, lys2ΔBgl, hom3-10, ade2Δ1, ade8*	Richard Kolodner
SCY003	RDKY3023 X RDKY2669	this study
SCY004	SCY003, *dun1Δ::URA3*	this study
SCY005	SCY004, *dun1Δ::URA3, GFPSml1::HIS3*	this study
SCY028	SCY003, *sml1Δ::TRP1*	this study
SCY037	*MATa, GFPSml1::HIS3*	this study
SCY047	*MATa, dun1Δ::URA3*	this study
SCY049	*MATa, dun1Δ::URA3, GFPSml1::HIS3*	this study
SCY082	SCY028, *rad53Δ::HIS3*	this study
SCY101	SCY028, *mec1Δ::HIS3, tel1Δ::URA3, Dun1-TAF::G418*	this study
SCY102	SCY028, *rad53Δ::HIS3, chk1Δ::URA3, Dun1-TAF::G418*	this study
SCY108	*MATa, sml1Δ::TRP1, Dun1-TAF::G418*	this study
SCY109	SCY028, *mrc1Δ::URA3, rad9Δ::HIS3, Dun1-TAF::G418*	this study
SCY105	*MATa, sml1Δ::TRP1, rad53Δ::HIS3, Dun1-TAF::G418*	this study
SCY106	*MATa, sml1Δ::TRP1, mec1Δ::HIS3, Dun1-TAF::G418*	this study
SCY112	*MATa, sml1Δ::TRP1, rad53Δ::HIS3, chk1Δ::URA3, Dun1-TAF::G418*	this study
SCY113	*MATa, sml1Δ::TRP1, chk1Δ::URA3, Dun1-TAF::G418*	this study
SCY116	*MATa, sml1Δ::TRP1, rad9Δ::HIS3, Dun1-TAF::G418*	this study
SCY117	*MATa, sml1Δ::TRP1, mrc1Δ::URA3, Dun1-TAF::G418*	this study
SCY122	*MATa, sml1Δ::TRP1, mrc1Δ::URA3, rad9Δ::HIS3, Dun1-TAF::G418*	this study
SCY125	*MATa, sml1Δ::TRP1, tel1Δ::HIS3, Dun1-TAF::G418*	this study
SCY126	SCY049, *Dun1-TAF::G418*	this study
SCY127	SCY049, *dun1-TAF-D328A::G418*	this study
SCY128	SCY049, *dun1-TAF-S195A::G418*	this study
SCY136	SCY049, *dun1-TAF-S10A::G418*	this study
SCY137	SCY049, *dun1-TAF-S139A::G418*	this study
SCY138	SCY049, *dun1-TAF-T380A::G418*	this study
SCY140	SCY037, *rad9Δ::URA3*	this study
SCY141	SCY037, *mrc1Δ::URA3*	this study
SCY152	*MATa, sml1Δ::TRP1, rad53Δ::HIS3*	this study
SCY156	*MATa, sml1Δ::TRP1, Rad53-TAF::G418*	this study
SCY157	*MATa, sml1Δ::TRP1, rad53-K227A D319A D339A::G418*	this study
SCY158	*MATa, sml1Δ::TRP1, rad53-T354A:G418*	this study
SCY159	SCY028, *Rad53::G418*	this study
SCY160	SCY028, *rad53-K227A D319A D339A::G418*	this study
SCY161	SCY028, *rad53-T354A::G418*	this study
SCY162	*MATa, sml1Δ::TRP1, Rad53::G418*	this study
SCY163	*MATa, sml1Δ::TRP1, rad53-K227A D319A D339A::G418*	this study
SCY164	*MATa, sml1Δ::TRP1, rad53-T354A::G418*	this study

Table 2.2 Plasmids used in this study

HZE1201	pGEX4T1-Sml1	this study
HZE1202	pFA6a-GFP-Sml1-KanMX6	this study
HZE1203	pFA6a-Dun1TAF-KanMX6	this study
HZE1204	pFA6a-Dun1TAF(S10A)-KanMX6	this study
HZE1205	pFA6a-Dun1TAF(S139A)-KanMX6	this study
HZE1206	pFA6a-Dun1TAF(S195A)-KanMX6	this study
HZE1207	pFA6a-Dun1TAF(T380A)-KanMX6	this study
HZE1208	pFA6a-Dun1TAF(D328A)-KanMX6	this study
HZE1209	pFA6a-Dun1TAF(R60A, N103A)-KanMX6	this study
HZE1210	pFA6a-Rad53-KanMX6	this study
HZE1211	pFA6a-Rad53(T354A)-KanMX6	this study
HZE1212	pFA6a-Rad53(K227A)-KanMX6	this study
HZE1213	pFA6a-Rad53TAF-KanMX6	this study
HZE1214	pFA6a-Rad53TAF(T354A)-KanMX6	this study
HZE1215	pFA6a-Rad53TAF(K227A, D319A, D339A)-KanMX6	this study
HZE1216	pET21a-ProtA-Rad53	this study
HZE1217	pET21a-ProtA-Rad53(T5A,T8A, T12A, T15A)	this study

Chapter 3: Reconstitution and characterization of adaptor protein Mrc1 mediated Rad53 activation by Mec1

3.1 Summary

Upon replication stress, signals from localized stalled replication forks are detected and amplified through replication checkpoint to provoke essential cellular responses. In *Saccharomyces ceravisiae*, the effector kinase Rad53, a human ortholog Chk2, plays the key role in replication checkpoint signaling. The activation of Rad53 depends on multiple proteins including upstream sensor kinase Mec1, a human ortholog ATR. Using a coupled phosphorylation assay including Rad53, we screened for proteins that could directly activate Rad53 in vitro. We report that Mrc1, a mediator for replication checkpoint, could collaborate with Mec1 to activate Rad53. This was further demonstrated using purified proteins to reconstitute Rad53 activation. Mrc1 was found to provide an over 70-fold stimulation of Rad53 activation by Mec1. This Mrc1 effect depends on its conserved C-terminal domain and its canonical phosphorylation by Mec1. Kinetic analysis showed that instead of a two-step linear pathway, the primary role of Mrc1 is to promote Rad53 phosphorylation by Mec1 by catalyzing the enzyme-substrate interaction between Mec1 and

Rad53. This study thus provides mechanistic insights into the role of adaptor proteins for DNA replication checkpoint activation.

3.2 Introduction

Rad53 and Cds1, orthologs of human Chk2, are the major effector kinases in DNA replication checkpoint in *S. ceravisiae* and *S. pombe* respectively. Upon activation, effector kinases control many cellular processes. Mrc1 appears to play a crucial role in the activation of Rad53 and Cds1. Under replication stress, Mrc1 is phosphorylated, possibly by Mec1 family kinases. Phosophorylated Mrc1 binds to Rad53 or Cds1 kinases and this binding is essential for the kinase activation. Mutations of the TQ sites of Mrc1 compromise Rad53 and Cds1 activation and abolish Cds1 binding to Mrc1 (Alcasabas et al., 2001; Tanaka and Russell, 2001). In addition to the recruitment of Rad53/Cds1 by Mrc1 for its activation, a direct phosphorylation of Rad53/Cds1 by Mec1/Rad3 has shown to be important for their activation. Analogous to the requirement of N-terminal TQ site phosphorylation of Chk2 by ATR in human (Matsuoka et al., 2000), the activation of Rad53/Cds1 in vivo requires phosphorylated TQ sites in their N-terminus, likely directly targeted by Mec1/Rad3 (Lee et al., 2003; Tanaka et al., 2001).

Given the many protein complexes are recruited at stall replication fork for the activation the DNA replication checkpoint, a key unresolved question is what is the minimal system in the DNA replication checkpoint required for

direct Rad53 activation? Second, what is the molecular mechanism of Rad53 activation by its upstream activators? Considering that Rad53 is capable of autophosphorylation and activation all by itself when over-expressed *in vitro*, one possible role of Mrc1 could be to promote Rad53 autophosphorylation directly. In this study, we developed an activity-based assay, consisting of Dun1, a downstream substrate of Rad53, and Sml1 as a substrate of Dun1, to quantitatively measure the activity of Rad53. Using this coupled kinase assay from Rad53 to Dun1 and Sml1, we screened for Mrc1 and its potentially associated factors to see whether they could directly activate Rad53. Our results showed that Mec1 and Mrc1 collaborate and constitute a minimal system in direct activation of Rad53, which led us to dissect the mechanisms in detail.

3.3 Results

3.3.1 Biochemical screen for Rad53 activators revealed a collaborative role of Mec1 and Mrc1

Many proteins are genetically implicated in Rad53 activation. To identify factors that may activate Rad53 directly, we developed a Rad53 activation system, consisting of inactive Rad53, inactive Dun1 and recombinant Sml1. As shown in Figure 3.1A, inactive Rad53 was purified using epitope tagged Rad53:6HisFLAG in *rad9Δ mrc1Δ* cells. Inactive Dun1 was purified using epitope tagged Dun1-TAF in *rad53Δ* cells. We have shown previously that

Dun1 is completely inactive in the absence of Rad53 {Chen, 2007 #84}. Because active Rad53 can efficiently phosphorylate and activate Dun1, which in turn would hyperphosphorylate Sml1 in a specific, sensitive and quantitative manner {Chen, 2007 #84}, we reasoned that any potential activator(s) of Rad53 could be identified, using this inactive Rad53-Dun1-Sml1 (RDS) system as a reporter.

Mrc1 is known to physically associate with Rad53, presumably through its phosphorylation by Mec1 {Alcasabas, 2001 #4}. Studies in *Saccharomyces ceravisiae* and Schizosaccharomyces pombe have suggested a potentially direct role of Mrc1 in Rad53 and Cds1 (Rad53 ortholog) activation {Tanaka, 2001 #26;Alcasabas, 2001 #4}. One possible hypothesis is that Mrc1 and its associated proteins may directly mediate Rad53 activation. Thus we chose to immunoprecipitate epitope tagged Mrc1-FLAG in *rad53Δ* cells using anti-FLAG immunoprecipitation approach. As a control, parallel anti-FLAG immunoprecipitation was performed using *rad53Δ* cells and *mec1Δ* cells. The immunoprecipitated samples were then added to the inactive RDS system to perform phosphorylation reaction with [γ32P] ATP. The amount of hyperphosphorylated Sml1 was quantified using scintillation counting. As shown in Figure 3.1B, the highest activity was observed for the immunoprecipitated sample from Mrc1-FLAG in *rad53Δ* cells (lane 8). This activity is reduced 10-fold to the basal level when inactive Rad53 was omitted in the kinase assay (see lane 5 in Fig. 3.1B). In contrast, anti-FLAG

immunoprecipitated samples from either *mec1Δ* cells or rad53Δ cells are less potent, showing a 5-fold and 2-fold reduction in the amount of hyperphosphorylated Sml1, respectively. Reproducible results were obtained in repeated experiments, indicating that there are unknown factors that co-purified with Mrc1 help Rad53 activation (compare lane 6 with lanes 7 and 8). Importantly, such factor is Mec1 dependent and Rad53-independent (comparing lanes 6 and 7), despite that no FLAG epitope tagged gene was present in *mec1Δ* and *rad53Δ* cells.

Next, the immunoprecipitated samples from these mutant cells were analyzed using Silver staining (see Fig. 3.1D). While most of the protein bands are common in all three samples, a distinct band with a MW over 250KD was seen only in lanes 2 and 3 and is absent in lane 1 where *mec1Δ* cells was used. This band was exercised from the gel and the protein in this band was identified as Mec1. To identify additional specific proteins that might be present in the immunoprecipitated samples, we used in-solution trypsin digest of the samples and analyzed them using mass spectrometry. This effort led to the identification of more than a hundred proteins (see Fig. 3.1E). While most of the proteins were identified in all three immunoprecipitated samples, suggesting that they are common contaminants to anti-FLAG resin, several proteins were reproducibly identified in these samples with known functions in the DNA damage checkpoint. Specifically, Mec1 and Ddc2 were found in both

samples immunoprecipitated from rad53Δ and Mrc1:FLAG*/rad53Δ* cells, Mrc1 was only found in the sample from Mrc1:FLAG/*rad53Δ* cells. Neither Mec1 nor Mrc1 was found in the sample from *mec1Δ* cells. In short, Mec1 was unexpectedly purified using anti-FLAG immunprecipitation. The observation that Mec1 and Mrc1 appear to have a synergistic effect in promoting Rad53 activation immediately provided the clue that perhaps Mec1 and Mrc1 alone could activate Rad53 (see Fig. 3.1C), while lack of either Mec1 in *mec1Δ* sample or Mrc1 in the *rad53Δ* sample compromised the activation of Rad53 and thus Dun1 dependent hyperphosphorylation of Sml1.

3.3.2 Development of an activity based assay for Rad53 using Dun1 and Sml1

The above observation that Mec1 and Mrc1 may act together to activate Rad53 promoted us to examine their effects in greater detail. To this end, it is necessary to have sufficient amounts of inactive Rad53 and inactive Dun1 while it is challenging to purify endogenously expressed Rad53 and Dun1 (see Fig. 3.1A). We chose to over-express recombinant Rad53 from E. coli, which is known to be active. As shown in Figure 3.2A, following an extended Lambda phosphatase treatment, recombinant Rad53 was dephosphorylated and showed a faster migration in the gel. Unpublished observation indicated that this Lambda phosphatase-dephosphorylated Rad53

has a similar activity compared to the endogenous Rad53 purified from rad9Δ mrc1Δ cells, thus it is considered inactive. To prepare inactive Dun1, Dun1 was over-expressed in rad53Δ cells and purified (see Fig. 3.2A). Next, we confirmed the activity of these purified kinases using Sml1 as a substrate. As shown in Figure 3.2B, only when active Rad53, inactive Dun1 and Sml1 were used, a characteristic gel-shift of the hyperphosphorylated Sml1 was found. The same amount of inactive Rad53 failed to cause appreciable hyperphosphorylation of Sml1.

Next, we examined how increasing amounts of Rad53 may affect Sml1 hyperphosphorylation, using either active or inactive Rad53. As shown in Figure 3.1E, from left to right, there is a two-fold increase in the amount of active or inactive Rad53. In general, the use of more Rad53 led to more hyperphosphorylated Sml1, regardless of their activity status. However, there is a striking difference between the amounts of active Rad53 and inactive Rad53 needed to achieve the same level of hyperphosphorylated Sml1. Quantification of the hyperphosphorylated Sml1 revealed an approximately 250-fold difference in concentration between active and inactive Rad53 to achieve the same amount of Sml1 hyperphosphorylation (see Fig. 3.2F). This allowed us to choose a concentration of inactive Rad53, i.e. 0.5nM, for an inactive Rad53-Dun1-Sml1 system. It should be noted that a similar amount of inactive Rad53 and Dun1 was used in the initial biochemical screen (see Fig. 3.1). As indicated in Figure 3.2F, at this concentration, active Rad53 is

capable of activating Dun1 for an almost complete Sml1 hyperphosphorylation. Thus, there is a sufficient dynamic range to detect any increase in Rad53 activity.

3.3.3 Reconstitution of Rad53 Activation by Mec1/Ddc2 and Mrc1 In Vitro

We examined the potential of Mec1/Ddc2 complex alone to activate Rad53. Mec1/Ddc2 was purified to homogeneity using the purification scheme incorporating anti-FLAG affinity purification (Figure 3.3A, see Experimental Procedure for details). Addition of increasing amount of this purified Mec1/Ddc2 complex to the inactive RDS system led to a noticeable increase of Sml1 hyperphosphorylation (see Fig. 3.3B). However, even at the highest concentration of Mec1/Ddc2 complex used (17 nM), the amount of hyperphosphorylated Sml1 is still much less than the use of 0.5nM active Rad53, which is the same amount as the inactive Rad53 used in this experiment. Further, this effect of Mec1/Ddc2 requires the presence of both inactive Rad53 and inactive Dun1, thus confirming the specificity of Rad53 activation by Mec1 (see Fig. 3.3C). In conclusion, the Mec1/Ddc2 complex alone did activate the inactive RDS system, albeit with a relatively poor efficiency.

To examine the effect of Mrc1, we chose a Mec1/Ddc2 concentration (0.13 nM) that is low enough to avoid any appreciable hyperphosphorylation of Sml1

by itself (see arrow in Fig. 3.3B). Recombinant Mrc1, either WT or the AQ mutant protein was purified from E.coli to homogeneity (see Fig. 3.3D). As shown previously {Alcasabas, 2001 #4}, the MRC1-AQ mutant is defective in checkpoint activation in vivo. We examined the effect of increasing amounts of either WT or AQ mutant protein of Mrc1 to inactive RDS in the presence of 0.13nM Mec1-Ddc2. As shown in Figure 3.3E, while addition of Mrc1-AQ mutant protein failed to cause any appreciable increase of Sml1 hyperphosphorylation, addition of Mrc1 WT protein led to a significant increase in Sml1 hyperphosphorylation. At the highest amount of WT Mrc1 used (>30 nM), a similar amount of hyperphosphorylated Sml1 was obtained compared to the use of active Rad53 as the positive control (see right lane in Fig. 3.3E). Compared to the absence of Mrc1, WT Mrc1 led to over 70-fold increase in the amount of Sml1 hyperphosphorylation, and this increase by the addition of Mrc1 is specific. Significant hyperphosphorylation of Sml1 was detected only in the phosphorylation reaction containing Mec1/Ddc2, WT Mrc1, inactive Rad53 and inactive Dun1. Omission of any one of these components or replacing WT Mrc1 by Mrc1-AQ mutant protein severely reduced Sml1 hyperphosphorylation (see Fig. 3.3F). This result demonstrated that the phosphorylation cascade from Mec1 to Rad53, Dun1 and Sml1 has been successfully reconstituted in vitro, with Mrc1 plays a critical role in mediating this process.

We then took a closer examination of the phosphorylation status of Mrc1, Rad53 and Dun1 in the reconstituted system (see Fig. 3.3G). As shown in lane 3 in Figure 3.3G, inactive Rad53 alone can autophosphorylate itself, leading to a shifted and phosphorylated Rad53. Addition of inactive Dun1 appears to suppress this Rad53 autophosphorylation and Dun1 becomes more phosphorylated in the same reaction (comparing lanes 2 and 3). Thus, Dun1 appears to have an effect to direct the activity of Rad53 to itself.

In vitro, Mrc1 is phosphorylated by Rad53. Comparison between lanes 4, 7 and 10 revealed a much higher level of Mrc1 phosphorylation in the presence of inactive Rad53, but not Rad53 kinase-dead (KD) mutant protein. In addition, there is a higher level of Rad53 phosphorylation, comparing lanes 2 and 7, suggesting that Mrc1 promotes Rad53 activation. Interestingly, addition of inactive Dun1 again suppressed the phosphorylation of both Mrc1 and Rad53, comparing lanes 7 and 13. In the same reaction, Dun1 became significantly more phosphorylated (see lane 13). As a result, Dun1 appears to direct Rad53 phosphorylation to itself and suppress the phosphorylation of Mrc1 and Rad53 in the process.

Finally, we specifically assayed a possible direct phosphorylation of Rad53 by Mec1. Because inactive Rad53 would become autophosphorylated, we chose to examine the phosphorylation of Rad53KD in the presence or absence of Mrc1 (comparing lanes 9 and 10), the result indicated that Mrc1 promoted the phosphorylation of Rad53KD by Mec1 (see lanes 9 and 10). As

expected, the use of Mrc1-AQ mutant protein greatly compromises not only its own phosphorylation, but also the phosphorylation of Rad53 and Dun1 (see lanes 5, 8, 11, 14 and 17). Consequently, the ability of Mrc1 to be phosphorylated by Mec1 is essential for the induced phosphorylation of Rad53 by Mec1.

3.3.4 The conserved Mrc1 C-terminal domain is essential for its Phosphorylation by Mec1/Ddc2 In Vitro and Rad53 activation In Vitro and *In Vivo*

With the reconstitution of Mrc1 mediated Rad53 activation by Mec1, it is possible to use this in vitro system to study the underlying mechanisms further. Recent studies have suggested the role of Mrc1 C-terminal region in stabilizing DNA polymerase Pol2 at stalled replication fork {Lou, 2008 #18}. Sequence alignment of Mrc1 homologs among yeast species showed a conserved C-terminal domain containing blocks of hydrophobic residues (see Fig. 3.4A). Secondary structure prediction suggested these blocks to be structured coil-coil domain. To ask what role it might have, short stretches of amino acid residues within this C-terminal region of Mrc1, 16-19 amino acids as indicated as T1, T2 and T3 (see Fig. 3.4A), was deleted from Mrc1. These internal deletion mutant proteins of Mrc1 were purified from E. coli and tested for their ability to mediate Rad53 activation by Mec1 (see Fig. 3.4B). As shown in Figure 3.4C, comparing WT and various C-terminal deletion mutants of

Mrc1, i.e., mutations to remove T1, T2 or T3 region of Mrc1, a partial loss of the Mrc1's ability to cause Sml1 hyperphosphorylation was found. Interestingly, deletion of both T2 and T3 regions of Mrc1 virtually eliminated its ability to cause Sml1 hyperphosphorylation (see Fig. 3.4C).

To further address what is the cause of the effect of C-terminal mutation of Mrc1, its phosphorylation by Mec1 was examined. As shown in Figure 3.4D, while WT Mrc1 was highly phosphorylated by Mec1 (see lane 2 in Fig. 4D), internal deletion of both T2 and T3 regions of Mrc1 greatly compromised its phosphorylation by Mec1, which is reduced to a level comparable to the non-specific phosphorylation of Mrc1-AQ mutant protein by Mec1. To address the *in vivo* relevance of the conserved C-terminal domain of Mrc1, these mutations were introduced to the endogenous MRC1 gene. Rad9 is known to act redundantly with Mrc1 for Rad53 activation, thus various C-terminal mutants of MRC1 were introduced in the rad9Δ background. As shown in Figure 3.4E, in the rad9Δ background, mutation to the C-terminal domain of Mrc1 led to a higher sensitivity to HU. The mrc1(ΔT2 ΔT3) rad9Δ double mutant is almost as sensitive as the rad9Δ mrc1Δ double mutant. Clearly, mutation to the C-terminal region of Mrc1 essentially impaired the ability of the cells to counter HU-induced replication stress.

Next, we asked whether HU induced phosphorylation of Rad53 is affected by these mutations. As shown in Figure 3.4F, HU-induced gel-shifts of both Mrc1 and Rad53 are not appreciably perturbed by mutations to remove

T1, T2 or T3 individually, deletion of both the T2 and T3 regions of Mrc1 greatly diminished the gel-shift of both mutant Mrc1 and Rad53, indicating that HU-induced Rad53 activation in vivo is compromised. Taken together, there is an interesting parallel between the relative severity of defects of various Mrc1 C-terminal mutants both in vivo and in vitro. Particularly, the *mrc1(ΔT2 ΔT3)* double mutant behaves essential as the Mrc1 AQ or the null mutant. In conclusion, the conserved C-terminal domain of Mrc1 is required for its ability to mediate Rad53 activation by Mec1 in vitro and in vivo.

3.3.5 Simultaneous requirement of Mec1 and Mrc1 towards maximum activation of Rad53

Two distinct models could be proposed to explain how Mrc1 could mediate Rad53 activation by Mec1 (see Fig. 3.5A). According to the two-step Model A, Mec1 first phosphorylates Mrc1, which in turn activates Rad53 in a step-wise fashion. Support of this model mostly arises from the observation that Rad53, when present in higher concentration, can autophosphorylate and activate itself. In this case, phosphorylated Mrc1 alone is sufficient to mediate a possible oligomerization and thus activation of Rad53. Alternatively, according to the second Model B, the role of Mrc1 phosphorylation by Mec1 is to facilitate Mec1 activation of Rad53 by either bringing Rad53 closer to Mec1 or stimulating Mec1 catalytic activity toward Rad53.

To address which model is more likely, we designed the following strategy: 10-fold more Mrc1 was first phosphorylated by 1-fold of Mec1 for an extended period of time. After this pre-incubation, one-tenth of the sample, containing 1-fold of phosphorylated Mrc1 and 1/10-fold of Mec1, will be added to inactivate RDS system, as the kinase reactions labeled A. If phosphorylated Mrc1 alone could mediate Rad53 activation according to Model A, hyperphosphorylated Sml1 will be observed. As a comparison, 1-fold of Mec1 will be freshly added in all the kinase reactions labeled as B. In this case, the same amount of Mec1 is assumed to be still required for activation of RDS, according to Model B. The actual experimental design is outlined in Figure 3.5B, three kinase reaction labeled as 1, 2 and 3 with either 1-fold Mec1, 10-fold Mrc1, or both were pre-incubated with ATP for an extended 3 hours, compared to the usual 30 minutes kinase reaction for Rad53 activation. After 3 hours, one tenth of each sample is added to RDS in all A-type kinase reactions or B-type kinase reactions with a freshly added 1-fold of Mec1. The results of Sml1 phosphorylation were shown in Figure 3.5C.

As shown in Fig. 3.5C, much more hyperphosphorylated Sml1 was detected in the B-type kinase reactions, as long as 1-fold of Mrc1 was present and regardless whether the Mrc1 was pre-phosphorylated by Mec1. Thus, a simultaneous presence of sufficient amounts of both Mec1 and Mrc1 is necessary for efficient Rad53 activation. Interestingly, comparison between the A-type kinase reactions indicated that pre-incubation between Mec1 and

Mrc1 did help to increase Sml1 hyperphosphorylation (comparing lanes 3 and 4); however, this effect is much smaller than the situations where Mec1 and Mrc1 are both present. We therefore concluded that Mec1 and Mrc1 are both required for efficient phosphorylation and activation of Rad53. The two-step sequential Model A appears to have a relatively minor role.

3.3.6 Mrc1 promotes enzyme-substrate interaction between Mec1/Ddc2 and Rad53

Following Model B, Mrc1 can either stimulate the catalytic activity of Mec1 towards Rad53 or promotes the enzyme-substrate interaction between Mec1 and Rad53. To address this question, kinetic analysis of the phosphorylation of Rad53KD by Mec1 was performed. As shown in Figure 3.6A, there is an approximately linear relationship between the amount of Rad53KD phosphorylation as a function of the time. The slop, representing the rate of Rad53KD phosphorylation by Mec1, is plotted as a function of Rad53KD concentration (see Fig. 3.6B). In the absence of Mrc1, as the concentration of Rad53KD increases, there is a gradual increase of the rate of Rad53KD phosphorylation by Mec1. Even at a high concentration of Rad53KD (>0.4 uM), it barely reaches saturation, which would correspond to a possible maximum velocity for Mec1 to phosphorylate Rad53KD. On the other hand, in the presence of (40nM) Mrc1, the rate of Rad53KD phosphorylation reaches a maximum at a much lower concentration of Rad53KD and becomes

independent of Rad53KD thereafter (see Fig. 3.6B). This analysis indicated that the apparent Km for the phosphorylation of Rad53KD by Mec1 is significantly reduced by Mrc1. The catalytic activity of Mec1; however, is not perturbed appreciably by Mrc1. This is also consistent with the observation in Figure 3.4D, where addition of Mrc1 to Mec1 does not change the ability of Mec1 to phosphorylate Ddc2 appreciably. Thus, the primary role of Mrc1 appears to bring Rad53 to Mec1 to facilitate its phosphorylation. Importantly, no other protein is involved, thus the effect of Mrc1 appears to be direct.

3.4 Discussion

Activation of effector kinases is the hallmark of replication checkpoint. Studies on the Chk2 family kinases have suggested evolutionarily conserved regulations for their activation. PIKK kinases have been shown to be involved in effector kinase activation, likely through direct phosphorylation {Lee, 2003 #36}. On the other hand, studies in yeast species have shown that adaptor proteins appear to play essential roles in effector kinase activation {Tanaka, 2001 #26;Alcasabas, 2001 #4}{Gilbert, 2001 #43}. However, a clear mechanistic insight into how PIKK kinases, together with adaptor proteins, regulate the activation of effector kinases remains elusive.

In this work, we have shown that adaptor protein Mrc1 promotes effector kinase Rad53 activation by PIKK kinase Mec1. We reconstituted the activation of Rad53 with purified proteins. In this reconstituted system, the

efficient activation of Rad53 requires both PIKK Mec1 and adaptor protein Mrc1. In our analysis, phosphorylated Mrc1 is not sufficient for the full activation of Rad53. On the other hand, Mec1 alone can partially activate Rad53, likely through its direct phosphorylation, only when Mec1 concentration is 30 fold higher than Rad53. Based on our initial estimation, the Km for the trimetric Mec1-Mrc1-Rad53 complex would be on the order of nM^2 range. The C-terminal domain of Mrc1 is important for its phosphorylation by Mec1 *in vitro* and Rad53 activation *in vivo*. It is possible that Mrc1 association with Mec1 through this conserved region. Kinetic analysis of Rad53 phosphorylation by Mec1 shows the apparent Km reduction but minor kcat increase with the addition of Mrc1. On the contrary, when PHSA-1 was used as Mec1 substrate, addition of Mrc1 showed no stimulating effect. Recent studies on TopBP1 and its homolog Dpb11, proteins involved in the initiation of DNA replication, suggested their role in direct stimulation of ATR and Mec1 catalytic activity {Kumagai, 2006 #62}{Navadgi-Patil, 2008 #58}{Mordes, 2008 #88}. Our study, on the other hand, showed a different mode of regulation in replication checkpoint signaling, specifically the activation of effector kinases through protein-protein interactions.

Our reconstitution reveals significant specificity of replication checkpoint signaling cascade. Omission of any one of the components in the reconstitution severely reduced Sml1 hyperphosphorylation. This specificity is further illustrated with the examination of Dun1, Rad53 and Mrc1

phosphorylation states. In the presence of Dun1, hyperphosphorylation of Rad53 and is reduced. In addition, with Mec1 and Mrc1, which result in hyperphosphorylation Rad53, the addition of Dun1 results in the reduction of both Rad53 and Mrc1 phosphorylation. We speculate that the reduction of Rad53 and Mrc1 autophosphorylation is due to the directed phosphorylation of Rad53 on Dun1 through Dun1 FHA domain binding to Rad53. Our previous studies and others have shown that defects in the Dun1 FHA binding to the phosphorylated N-terminal TQ sites of Rad53 compromises Dun1 activation *in vitro* and *in vivo* {Lee, 2003 #36}{Chen, 2007 #84}. Mrc1 AQ mutant is incompetent in activating Rad53, likely through the abolishment of Mrc1 phosphorylation by Mec1 and consequently Mrc1 binding to Rad53 FHA1 domain. Importantly, the presence of Mrc1 enhances the phosphorylation of Rad53 by Mec1, including its N-terminal TQ sites. In S. pombe, it has been suggested that phosphorylated N-terminal TQ sites could cause oligomerization of Cds1 through FHA domain binding in trans, and then lead to the auto-activation of Cds1 {Xu, 2006 #44}. Though the same mechanism that may promote Rad53 auto-activation remains to be tested. In brief, the chain of protein-protein interactions in mediating a step-by-step activation of replication checkpoint kinases initiated from Mel-Ddc2 association with Mrc1 could contribute to the specificity of signaling cascade both in vitro and in vivo. We believe that this minimum reconstituted system for the activation of Rad53

provides a valuable tool for further studies on signaling specificity in replication checkpoint.

Another adaptor protein Rad9, in parallel with Mrc1, has also been implicated in mediating Rad53 activation. Studies on Rad9 have suggested its role in inducing Rad53 phosphorylation by Mec1 {Sweeney, 2005 #90}. However, in our initial screening of Rad53 activator, we could never detect any Rad9 stimulating effect. It can be due to the difference in the specificity of Mrc1 and Rad9 association with Mec1. Though we cannot exclude the possibility that other proteins associated with Rad9 may necessary for specific activation of Rad53.

An intriguing question remains to be tested is how DNA and possibly other factors at replication fork regulate Rad53 activation. Mrc1 is a replication fork protein. It preferentially associates with fork like DNA structures. The extended model from our current work would be that the fork like DNA structure recruits both Mec1 and Mrc1 through RPA-coated single stranded DNA and the DNA fork junction respectively, and this recruitment results in a synergistic stimulation of Rad53 activation. Our initial test on the model didn't show any stimulating effect with the addition of fork like DNA with RPA. It seems likely that additional factors localized at stalled replication fork would be needed for DNA dependent Rad53 activation and remains to be identified.

3.5 Methods

3.5.1 Strains & plasmids

Standard yeast growth and genetic methods are used in this work. All the yeast strains are derived from the diploid of SCY003. Vector pB504 (Mec1/GST-Ddc2) for Mec1-Ddc2 overexpression is a kind gift from Dr. Peter Burgers. For Dun1 overexpression in yeast, DUN1 is cloned into PYES plasmid with a ProteinA tag followed by a Precission Protease cleavage site at its N-terminus. RAD53 wild type, kinase dead, and MRC1 were cloned into Pet21 plasmind with a ProteinA tag followed by a Precission Protease cleavage site at its N-terminus and a 6XHis tag at its C-ternimus.

3.5.2 Partial Purification of Mrc1 and Mass Spectrometry

All purification steps were performed at 4 degree. 2 liters of cell were grown in YPD media to log phase (OD600 ~ 0.8). Spheroplasts were performed as described [18]. Extract was prepared from spheroplasts in 10 ml buffer A (50 mM Tris-HCl 7.5, 150mM NaCl, 1mM DTT, 0.1% Tween 20, 5mM EDTA, 1mM PMSF, 1.5 μM pepstatin A, 1μM leupeptin, 0.2mM benzamidine, 5mM β-glycerophosphate, 5mM sodium fluoride) by sonication and clarification at 70,000 rpm in a MLA80 rotor for 10 minute. 200 μl anti-FLAG M2 affinity resin (Sigma) was added to 10ml extract (~30μg/μl protein) and the bead/extract mix was rotated for 3 hours. The column was then washed with

15 bead volume of TBSD (50 mM Tris-HCl 7.5, 150mM sodium chloride, 1mM DTT, 0.1% Tween 20) and proteins was eluted with 1 bead volume of TBSD containing 10% glycerol and 200 µg/ml 3X FLAG peptide (Sigma) for 1 hour at room temperature. Elution equivalent to 0.5 liter cell was prepared for mass spectrometry analysis [19].

3.5.3 Tandem Affinity Purification of epitope tagged endogenous Rad53 and Dun1

2 liters of cell were grown in YPD media to log phase and broken in an ice-cooled bead beater (Hamilton Beach/Proctor-Silex, Inc.) in 40ml buffer A. Crude extracts were clarified by centrifugation at 15,000 rpm in a JA-25.50 rotor for 30 minutes and added to ~100 µl of anti-FLAG M2 resin and IgG Sepharose 6 Fast Flow resin (GE Healthcare) for the immunoprecipitation of Rad53-HisFLAG and Dun1-FLAG-TEV-ProteinA respectively. The bead/extract mix was rotated for 3 hours and the column was washed with 5 bead volume of TBSD supplemented with 1M sodium chloride followed by wash with 15 bead volume of TBSD (standard wash step). Rad53-HisFLAG was eluted with 2 bead volume TBSD containing 200 µg/ml 3X FLAG peptide and bound to 20 µl Ni-NTA resin (Qiagen) for 2 hours. The Ni-NTA column was washed with 15 bead volume TBSD and Rad53-HisFLAG was eluted with 4 bead volume of TBSD containing 10% glycerol and 200 mM imidazole. Dun1-FLAG-TEV was eluted by incubating with 2 bead volume TBSD

containing 10 unit of TEV protease for 2 hours at 30 degree and the supernatant was added to 20 µl anti-FLAG M2 resin for 2 hours. The anti-FLAG M2 column was washed with 15 bead volume TBSD and Dun1-FLAG-TEV was eluted with 4 bead volume of TBSD containing 10% glycerol and 200 µg/ml 3X FLAG peptide for 1 hour at room temperature. Both Rad53-HisFLAG and Dun1-FLAG-TEV purification resulted in the protein concentration of ~20 ng/µl.

3.5.4 Tandem Affinity Purification of recombinant Rad53 and recombinant Mrc1

BL21 cell was used as a host to overexpress ProteinA-PP-Rad53-His and ProteinA-PP-Rad53KD-His using standard protocol. Extract was prepared from 2 liters of cells in 20ml of buffer A by sonication and clarification at 30,000 rpm in a JA-25.50 rotor for 30 minute. 250 µl IgG Sepharose 6 Fast Flow resin was added to extract and the bead/extract mix was rotated for 2 hours and the column was washed with standard step. For the purification of active PP-Rad53-His, PP-Rad53-His was eluted with 3 bead volume TBSD containing 10 units of precission protease (Amersham Biosciences) overnight and the supernatant was bound to 100 µl Ni-NTA for 2 hours. The Ni-NTA column was washed with 15 bead volume TBSD and PP-Rad53-His was eluted with 2 bead volume of TBSD containing 200 mM imidazole. Elution was dialyzed with TBSD supplemented with 10% glycerol. The final PP-Rad53-His concentration

was around 500ng/ul. For the purification of inactive PP-Rad53-His, all the steps were the same except the addition of the inaction step after the wash of Sepharose 6 Fast Flow resin. To inactive/dephosphorylate Rad53, Sepharose 6 Fast Flow column was incubated with 1000 units of λ protein phosphatase (New England BioLabs Inc.) in one bead volume TBSD supplemented with 5mM magnesium chloride and 2% glycerol for 12 hours at room temperature. The purification of ProtainA-PP-Mrc1-His was analogous to described above except the protein expression was induced at 13 degree overnight.

3.5.5 Overexpression and Purification of Dun1 and Mec1/Ddc2

PYES-ProteinA-PP-Dun1 was transformed in S. cerevisiae strain SCY152. 100ml of cells were grown in CSM-Ura 2% glucose to an OD600 of 1.5. Cells were pelleted and resuspended to CSM-Ura, 2% galactose, 0.1% glucose and grew for 12 hours. Extract was prepared by breaking cells in 10ml buffer A through vortex (Vortex-Genie 2, Scientific Industries, Inc.), centrifuging at 13,200 rpm in a F45-24-11 rotor for 10 minutes. 100 µl IgG Sepharose 6 Fast Flow resin was added to extract and the bead/extract mix was rotated for 2 hours. The column was washed with standard step. PP-Dun1 was eluted by incubating with 2 bead volume TBSD containing 10% glycerol, and 5 unit precission protease overnight. Final PP-Dun1 protein concentration was around 500 ng/µl.

S. cerevisiae strain SCY001, transformed with plasmid pBL504

(Mec1/GST-Ddc2), was grown and induced with galactose using conditions analogous to described above. 12 liters of cells were broken in an ice-cooled bead beater in 300ml buffer B (buffer A plus 0.01% NP40) and clarified by centrifugation at 15,000 rpm in a JA-25.50 rotor for 30 minutes. Proteins were precipitated with ammonium sulfate to 55% saturation, and the precipitate collected at 15,000 rpm for 30 min. The protein pellet was resuspended in 30 ml of buffer B and added to 3ml of anti-FLAG M2 resin. The bead/extract mix was rotated for 4 hours followed by standard wash. Proteins were eluted with 3 bead volume TBSD containing 100 µg/ml 3X FLAG peptide. 300 ul of Glutathione Sepharose 4 Fast Flow resin (Amersham Biosciences) was added to the supernatant and the bead/supernatant was rotated overnight. The column was washed with standard step and Mec1/Ddc2 was eluted by incubating with 2 bead volume TBSD containing 50 unit precission protease for 4 hours. The enzymatic digest was loaded onto a 1 ml heparin-agarose column, washed with 10ml of TBSD and eluted with 1 ml of TBSD containing 500mM sodium chloride. Finally, elution was dialyzed with TBSD supplemented with 10% glycerol. Final Mec1/Ddc2 protein concentration was around 100 ng/µl.

3.5.6 Kinase reaction

In a typical kinase assay, 50 mM Tris, pH7.5, 150mM NaCl, 0.1% Tween 20, 0.2 mM ATP, 10mM $MgCl_2$, 10 µCi of ^{32}P-ATP were used. 30

minutes kinase reaction at 30 °C was always used if not mentioned otherwise.

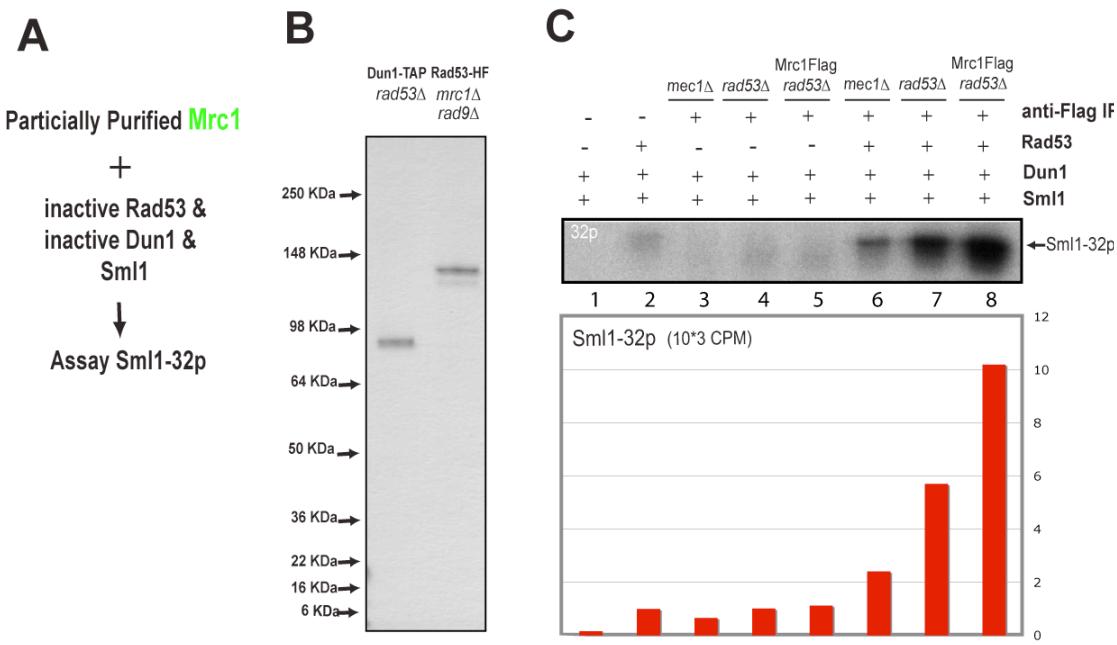

Figure 3.1(A-C) An In Vitro Assay for Detecting Mrc1's Effect on Rad53 Activation

(A) the schematic of the in vitro assay.

(B) silver staining of epitope tagged endogenous Rad53 and Dun1 purification from Rad53:HISFLAG/*rad9Δ,mrc1Δ* and Dun1:TAP/*rad53Δ* respectively.

(C) anti-FLAG immunoprecipitation from Mrc1:FLAG/*rad53Δ* and *rad53Δ* strains induce the activation of Rad53. Anti-FLAG immunoprecipitation from *mec1Δ, rad53Δ*, and Mrc1:FLAG/*rad53Δ* strains were tested for their ability to activate Rad53 using the in vitro screening phosphorylation assay. Phosphorylation reactions were all carried out at 30°C for 30 minutes. Twenty micro-liters of reactions were analyzed by SDS-10%-PAGE followed by scintillation quantification if not mentioned otherwise (see Experimental Procedures for details). Proteins when present in the phosphorylation reactions were the following: ~0.5nM of endogenous Rad53, ~0.85nM of endogeous Dun1, 3μM Sml1 and 1% of Anti-FLAG immunoprecipitations from two liters of cell culture. These results are representative of three independent experiments.

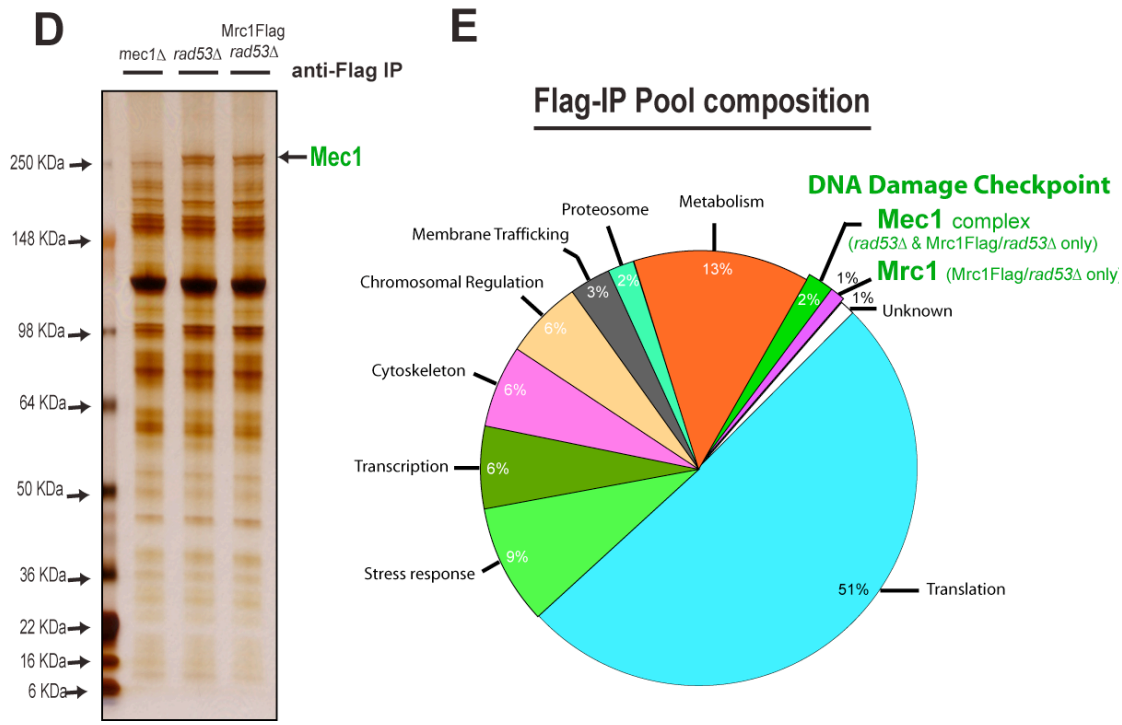

Figure 3.1(D,E) An In Vitro Assay for Detecting Mrc1's Effect on Rad53 Activation

(D) silver staining of 10% of anti-FLAG immunoprecipitations from two liters of *mec1Δ*, r*ad53Δ*, and Mrc1:FLAG*/rad53Δ* strains.

(E) Annotation-based classification of proteins identified by mass spectrometry of anti-FLAG immunoprecipitation. The 126 proteins that showed >10 identifications and >15% sequence coverage are represented in the pie chart (see also Table S1).

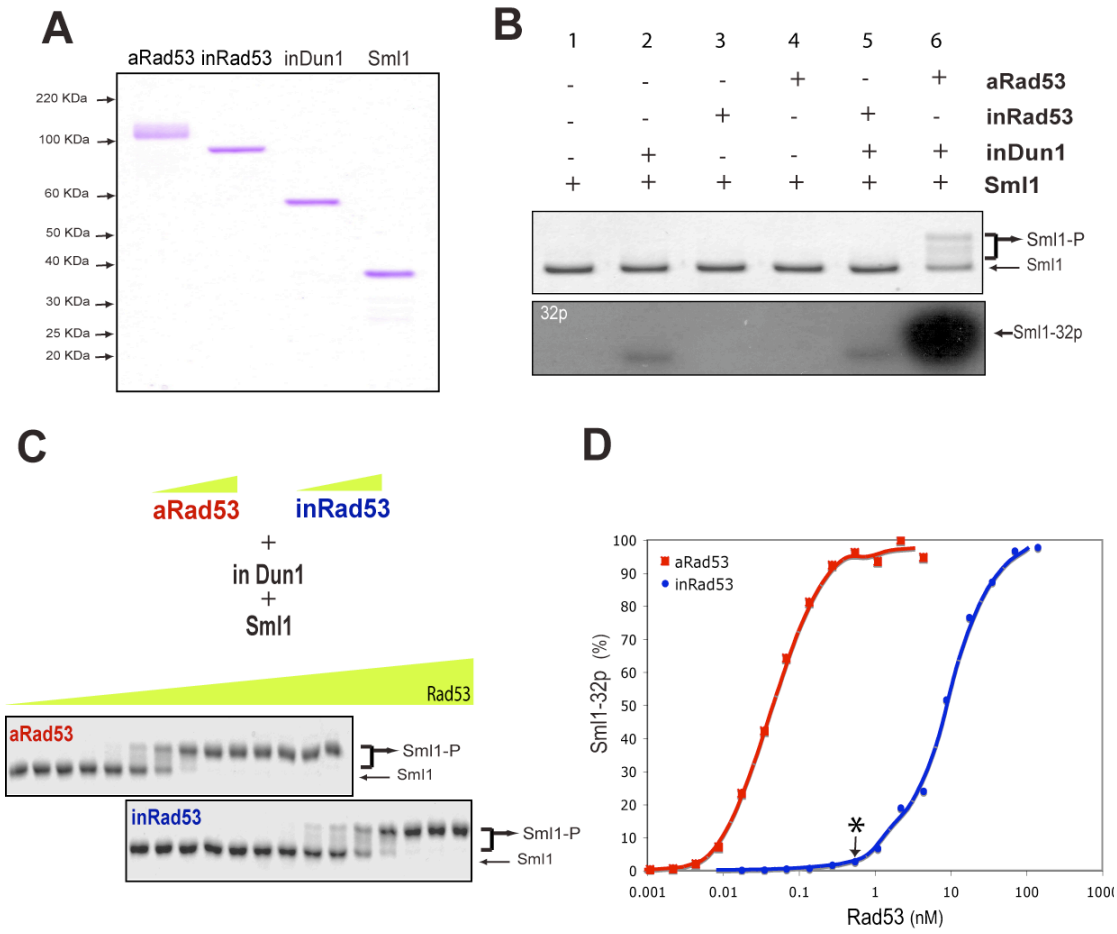

Figure 3.2 Development of Rad53 Activity Based Assay for quantifying effects of Rad53 activators

(A) Coomassie staining of purified proteins for Rad53 activity based assay: active Rad53 (aRad53), inactive Rad53 (inRad53), inactive Dun1 (inDun1) and Sml1 (see Experimental Procedures for purification details).

(B) Rad53 and Dun1 specificity for Sml1 hyperphosphorylation. Proteins when present in the phosphorylation reactions were the following: 17pM aRad53 and inRad53, 8.5nM inDun1, and 3μM Sml1.

(C) Comparison of activities of inRad53 and aRad53. Titrations of inRad53 and aRad53 were subjected to phosphorylation reactions with 8.5nM inDun1 and 3μM Sml1.

(D) Quantification of Sml1 phosphorylation from (C). The concentration of inRad53, 0.5nM, marked with asterisk was chosen for the Rad53 Activity Based Assay -RDS. All the values of RDS are normalized with the signal of saturated hyperphosphorylation of Sml1.

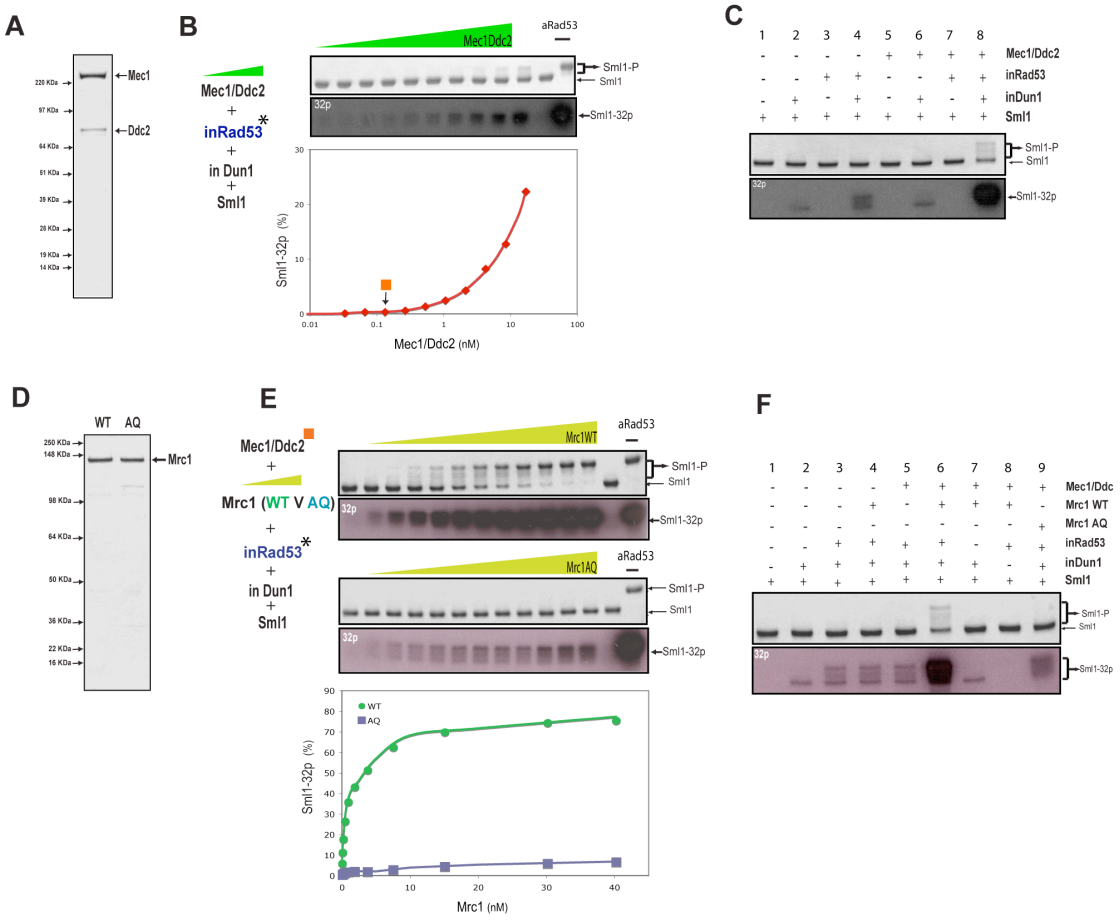

Figure 3.3(A-F) Reconstitution of Rad53 Activation using purified Mec1-Ddc2 and Mrc1

(A) Coomassie staining of purified Mec1-Ddc2 complex (see Experimental Procedure for details).

(B) Activation of inRad53 by Mec1. Titrations of Mec1-Ddc2 were tested for inRad53 activation using RDS. The concentration of Mec1-Ddc2, 0.13nM, marked with square was chosen for all the later tests of Mrc1 effect.

(C) Mec1-Ddc2 specificity for inRad53 activation. Proteins when present in the phosphorylation reactions were the following: 0.13nM Mec1-Ddc2, 0.5nM inRad53, 8.5nM inDun1, and 3μM Sml1.

(D) Commassie staining of purified wild-type and AQ mutant of recombinant Mrc1 (see Experimental Procedure for details).

(E) Activation of inRad53 by Mrc1 and Mec1-Ddc2. Titrations of wild-type and AQ mutant of Mrc1 were tested for inRad53 activation using RDS in the presence of 0.13nM Mec1-Ddc2.

(F) Mrc1 specificity for inRad53 activation. Proteins when present in the phosphorylation reactions were the following: 0.13nM Mec1-Ddc2, 0.6nM Mrc1 (wild-type and mutant), 0.5nM inRad53, 8.5nM inDun1, and 3μM Sml1.

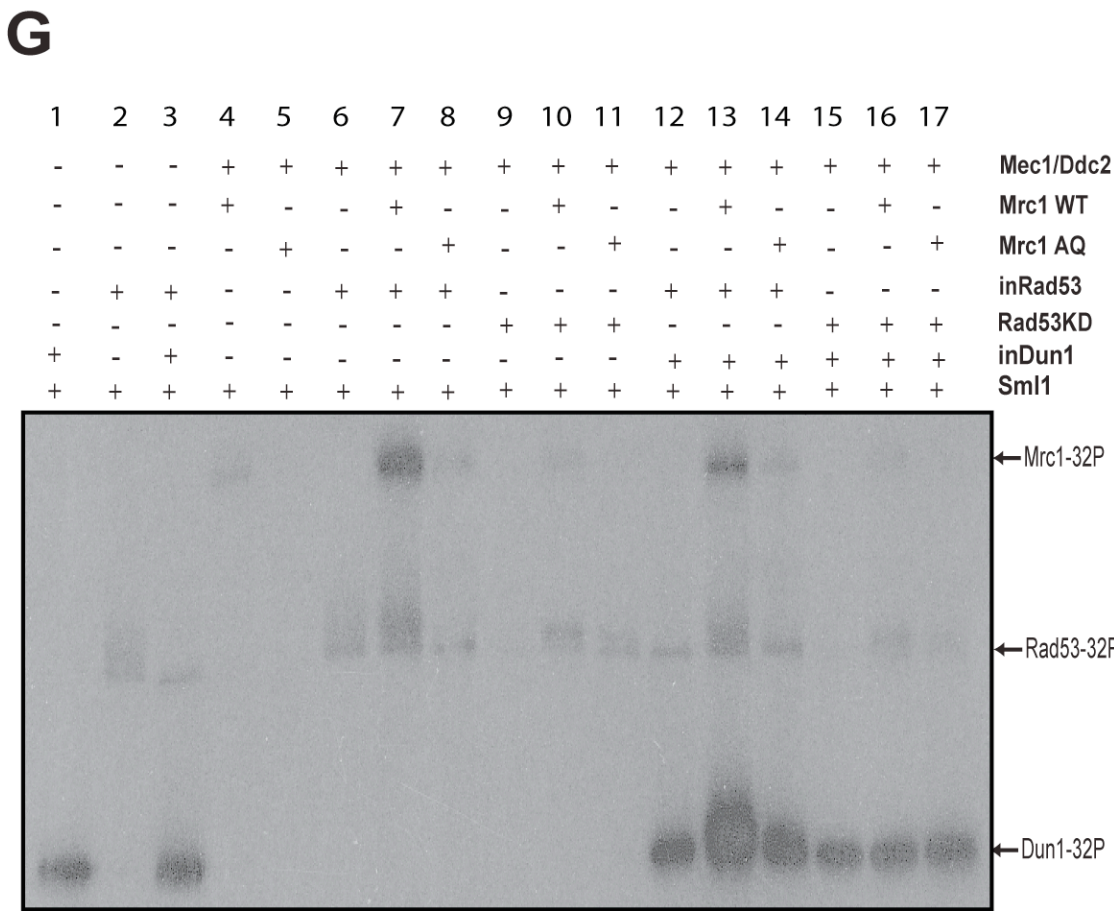

Figure 3.3(G) Reconstitution of Rad53 Activation using purified Mec1-Ddc2 and Mrc1

(G) Phosphorylation states of Mrc1, inRad53, inDun1 and Rad53KD in the reconstituted system. Kinase reactions were carried out as described in (F) other than 0.5nM of recombinant Rad53KD. Fifty micro-liters of reactions were analyzed by SDS-10%-PAGE followed by phosphorimaging.

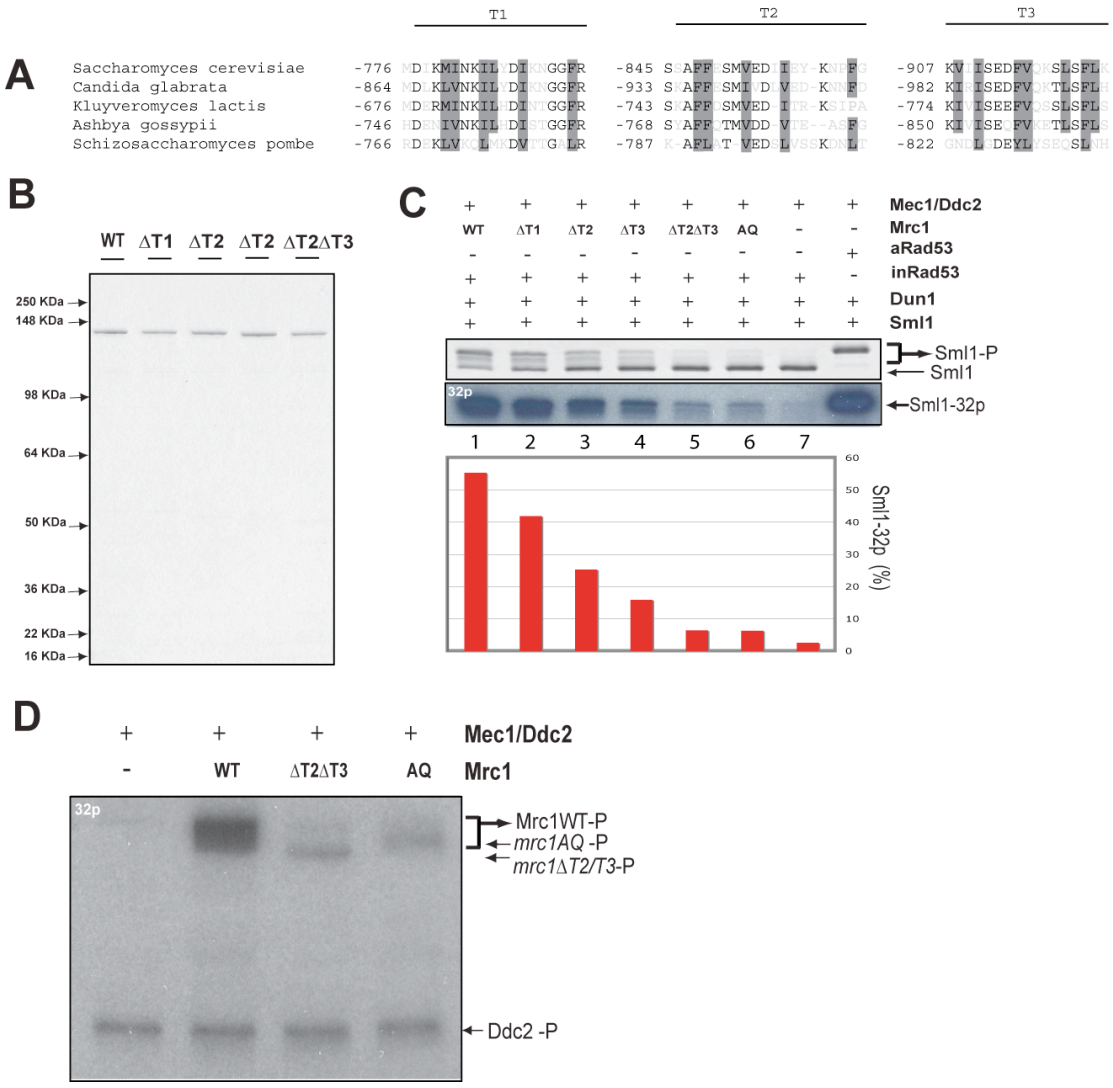

Figure 3.4(A-D) Mrc1 Carboxyl-terminus Domain is required for its Phosphorylation by Mec1-Ddc2 In Vitro and Rad53 Activation In Vivo

(A) Alignment of three conserved blocks, T1(776-794), T2(845-864), T3(907-923), from carboxyl-terminus domain of Mrc1 with the corresponding sequences of four related yeast species including Schizosaccharomyces pombe. Conserved residues with similar properties are marked with black, while hydrophobic residues are indicated with gray background.

(B) Commassie staining of purified mutants of recombinant Mrc1 (see Experimental Procedure for details).

(C) Mutations on Mrc1 carboxyl-terminus domain abolishes inRad53 activation in vitro. Mrc1 wild-type and mutants (ΔT1, ΔT2, ΔT3, ΔT2ΔT3, and AQ) were tested with RDS. Proteins when present in RDS are the following: 0.13nM Mec1-Ddc2, and 2.5nM Mrc1.

(D) Mrc1 mutants (ΔT2ΔT3 and AQ) phosphorylation by Mec1-Ddc2 is diminished in vitro. Proteins when present in phosphorylation reactions are the following: 16nM Mec1-Ddc2, and 160nM Mrc1.

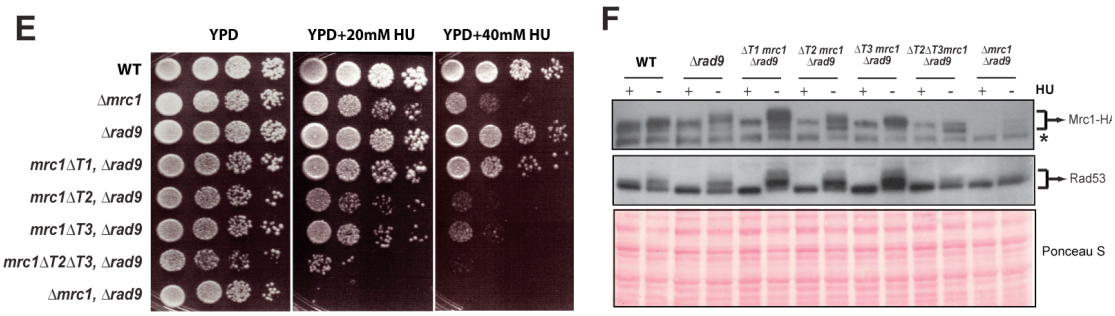

Figure 3.4(E,F) Mrc1 Carboxyl-terminus Domain is required for its Phosphorylation by Mec1-Ddc2 In Vitro and Rad53 Activation In Vivo

(E) Mrc1 carboxyl-terminus domain mutations show hydroxyurea sensitivity. Five fold dilutions of logarithmically growing cell were spotted on YPD plates and the ones containing 20mM and 40mM hydroxyurea, and incubated at 30°C for 3 days.

(F) Mrc1 and Rad53 phosphorylation in vivo depends on Mrc1 carboxyl-terminus domain. *S. ceravisiae* wild-type, or mutant cells were incubated in the absence (-) or presence (+) of 100mM hydroxyurea for 2 hours at 30°C. The phosphorylation states of Mrc1 (top panel) and Rad53 (middle panel) were analyzed by SDS-10%-PAGE and Western blotting with anti-HA (Roche) and anti-Rad53 (Santa Cruze Biotechnology, Inc.) antibodies respectively. Bottom panel is the Ponceau S staining of the Western blotting film.

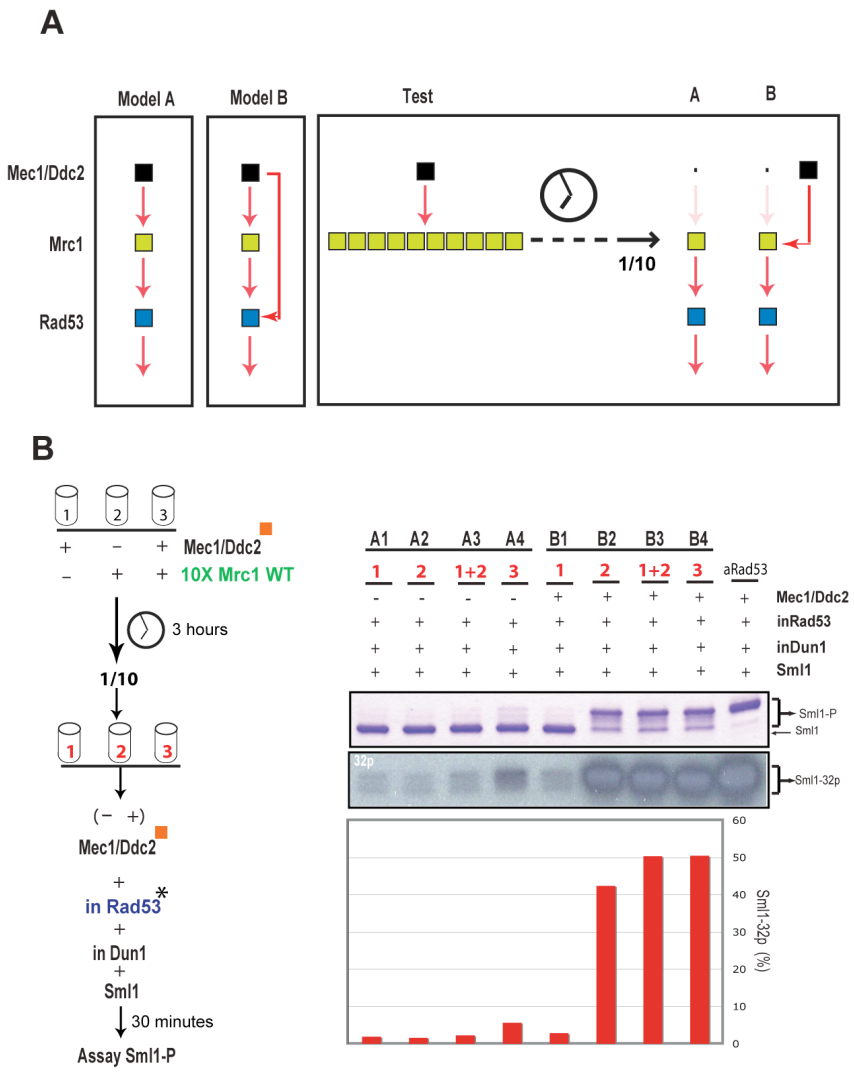

Figure 3.5 Tests of Signaling Models for the Activation of Rad53

(A) the schematic of model testing for Rad53 activation. Model-A and Model-B represent linear and feed-forward signaling for Rad53 activation respectively. To test which model plays the major role in activating Rad53 in our reconstituted system, concentrated Mrc1 is phosphorylated by Mec1-Ddc2 for a prolonged period followed by dilution so that Mec1 is limiting. Diluted samples are subjected to RDS test in the absence (A) or presence (B) of freshly added Mec1-Ddc2. If the Sml1 phosphorylation signal from (A) is similar to (B), then Model-A is preferred. If the RDS signal from (A) is much greater than (B), then Model-B is preferred.

(B) Model-B is preferred. Three phosphorylation reactions (tube 1, 2, and 3) were performed for three hours with 0.13nM Mec1-Ddc2 or 25nM Mrc1 when present (left panel). Samples were diluted by ten fold and subjected to RDS in the absence (A1-4) or presence (B1-4) of 0.13nM Mec1-Ddc2 (right panel). Model-B is preferred (right panel).

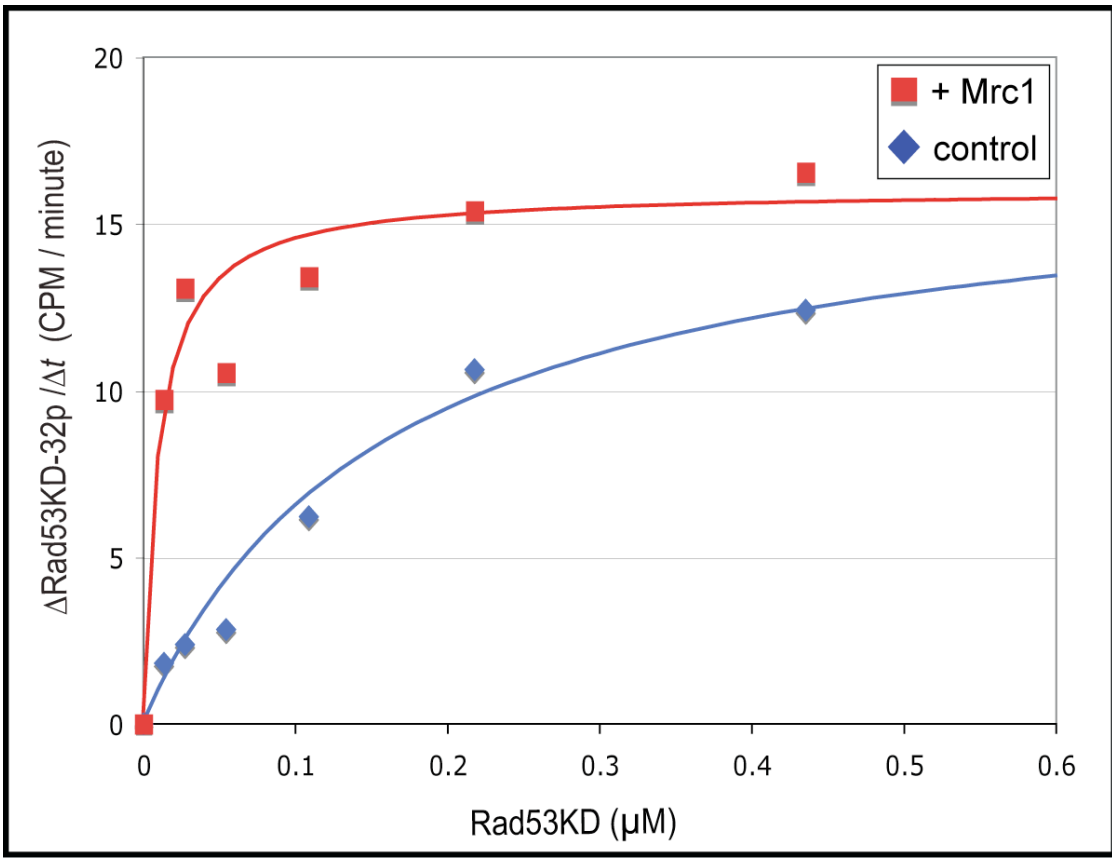

Figure 3.6 Mrc1 catalyzes stronger Association between Mec1-Ddc2 and Rad53KD

(A) Michaelis-Menten plots of initial rates of Rad53KD phosphorylation by Mec1-Ddc2 in the absence (blue) or presence (red) of 40nM Mrc1. The solid lines are nonlinear least-squares fits of the data to the Michaelis-Menten equation. The data shown are representive of three independent determinations.

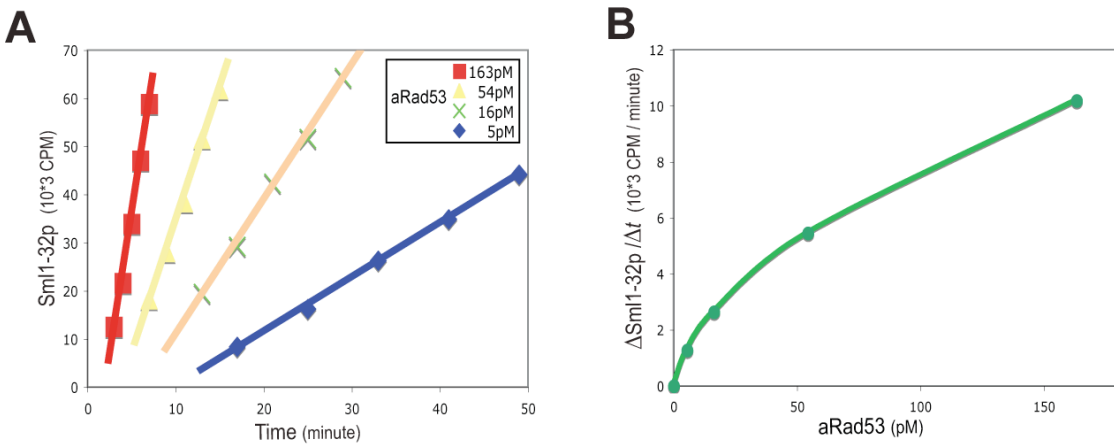

Figure S3.1 Development of Rad53 Activity Based Assay for quantifying effects of Rad53 activators

(A) Comparison of activities of inRad53 and aRad53. Titrations of inRad53 and aRad53 were subjected to phosphorylation reactions with 8.5nM inDun1 and 3μM Sml1.

(B) Quantification of Sml1 phosphorylation from (A). The concentration of inRad53, 0.5nM, marked with asterisk was chosen for the Rad53 Activity Based Assay. All the values of RABA are normalized with the signal of saturated hyperphosphorylation of Sml1.

A

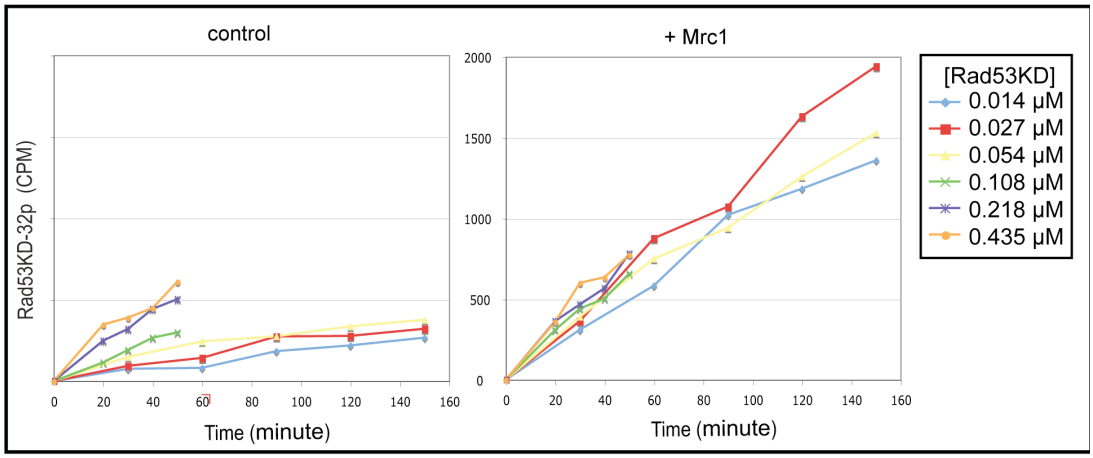

B

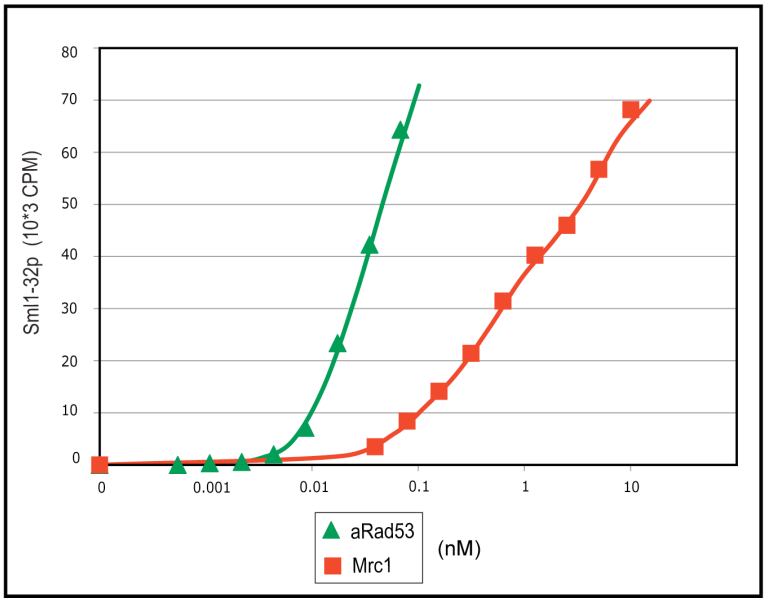

Figure S3.2 Mrc1 catalyzes stronger Association between Mec1-Ddc2 and Rad53KD

(A) Kinetics of Rad53KD phosphorylation by 0.13nM Mec1-Ddc2 in the absence (left) and presence (right) of 40nM Mrc1.

(B) Comparison of the Sml1 phosphorylation between Figure3.2D and Figure3.3E

Table 3.1 Composition of Flag immunoprecipitation

Systematic Name	Standard Name	% Coverage	*mec1Δ*	*rad53Δ*	*Mrc1:FLAG/rad53Δ*
DNA damage checkpoint					
YAR007C	**RFA1**	25	-	+	+
YBR136W	**MEC1**	32	-	+	+
YCL061C	**MRC1**	15	-	-	+
YDR499W	**LCD1**	25	-	+	+
Metabolism					
YLR044C	PDC1	28	+	+	+
YLR058C	SHM2	28	+	+	+
YLR180W	SAM1	39	+	+	+
YKL182W	FAS1	15	+	+	+
YPL110C	YPL110C	47	+	+	+
YAL038W	CDC19	48	+	+	+
YGR192C	TDH3	70	+	+	+
YGR254W	ENO1	50	+	+	+
YIL107C	PFK26	50	+	+	+
YKL060C	FBA1	31	+	+	+
YML056C	IMD4	25	+	+	+
YLR432W	IMD3	21	+	+	+
YGL009C	LEU1	76	+	+	+
YDR502C	SAM2	32	+	+	+
YOL055C	THI20	57	+	+	+
YML123C	PHO84	16	+	+	+
Chromosomal regulation					
YKL022C	CDC16	33	+	+	+
YBL002W	HTB2	45	+	+	+
YBR009C	HHF1	52	+	+	+
YMR247C	YMR247C	42	+	+	+
YFL037W	TUB2	31	+	+	+
YOL145C	CTR9	60	+	+	+
YMR076C	PDS5	48	+	+	+
Cytoskeleton					
YDL143W	CCT4	49	+	+	+
YDR188W	CCT6	62	+	+	+
YDR212W	TCP1	68	+	+	+
YIL142W	CCT2	73	+	+	+
YJL008C	CCT8	57	+	+	+
YJL014W	CCT3	51	+	+	+
YJL111W	CCT7	64	+	+	+
YJR064W	CCT5	68	+	+	+
Stress response					
YPL106C	SSE1	45	+	+	+
YAL005C	SSA1	69	+	+	+
YBL047C	EDE1	15	+	+	+
YHL007C	STE20	36	+	+	+
YHR082C	KSP1	28	+	+	+
YHR111W	UBA4	48	+	+	+
YLL024C	SSA2	22	+	+	+
YLR150W	STM1	59	+	+	+
YLR259C	HSP60	20	+	+	+
YML028W	TSA1	54	+	+	+
YNL064C	YDJ1	28	+	+	+

Table 3.1 continued

Proteosome					
YDL007W	RPT2	29	+	+	+
YDR394W	RPT3	26	+	+	+
YHR027C	RPN1	16	+	+	+
Transcription					
YBR247C	ENP1	34	+	+	+
YBR279W	PAF1	68	+	+	+
YGL207W	SPT16	25	+	+	+
YGL244W	RTF1	53	+	+	+
YJL148W	RPA34	44	+	+	+
YLR418C	CDC73	65	+	+	+
YOR123C	LEO1	39	+	+	+
YOR310C	NOP58	18	+	+	+
Translation					
YBL027W	RPL19B	46	+	+	+
YBL072C	RPS8A	36	+	+	+
YBR031W	RPL4A	56	+	+	+
YBR048W	RPS11B	42	+	+	+
YBR118W	TEF2	58	+	+	+
YBR181C	RPS6B	44	+	+	+
YBR189W	RPS9B	54	+	+	+
YBR191W	RPL21A	49	+	+	+
YDL075W	RPL31A	48	+	+	+
YDL082W	RPL13A	57	+	+	+
YDL083C	RPS16B	41	+	+	+
YDL136W	RPL35B	35	+	+	+
YDL229W	SSB1	70	+	+	+
YDR064W	RPS13	52	+	+	+
YDR385W	EFT2	25	+	+	+
YDR418W	RPL12B	61	+	+	+
YDR447C	RPS17B	51	+	+	+
YDR450W	RPS18A	40	+	+	+
YDR471W	RPL27B	50	+	+	+
YER074W	RPS24A	51	+	+	+
YER165W	PAB1	27	+	+	+
YFR031C-A	RPL2A	46	+	+	+
YGL030W	RPL30	68	+	+	+
YGL031C	RPL24A	32	+	+	+
YGL076C	RPL7A	59	+	+	+
YGL099W	LSG1	22	+	+	+
YGL103W	RPL28	40	+	+	+
YGL123W	RPS2	30	+	+	+
YGL135W	RPL1B	47	+	+	+
YGL147C	RPL9A	50	+	+	+
YGR027C	RPS25A	40	+	+	+
YGR034W	RPL26B	36	+	+	+
YGR085C	RPL11B	36	+	+	+
YGR118W	RPS23A	34	+	+	+
YGR159C	NSR1	32	+	+	+
YHL001W	RPL14B	49	+	+	+
YHL033C	RPL8A	53	+	+	+

Table 3.1 continued

YHR203C	RPS4B	41	+	+	+
YIL133C	RPL16A	30	+	+	+
YIL148W	RPL40A	25	+	+	+
YJL177W	RPL17B	34	+	+	+
YJL190C	RPS22A	59	+	+	+
YJR123W	RPS5	19	+	+	+
YLL045C	RPL8B	18	+	+	+
YLR029C	RPL15A	41	+	+	+
YLR075W	RPL10	49	+	+	+
YLR185W	RPL37A	24	+	+	+
YLR340W	RPP0	33	+	+	+
YLR441C	RPS1A	54	+	+	+
YLR448W	RPL6B	53	+	+	+
YMR194W	RPL36A	53	+	+	+
YMR242C	RPL20A	46	+	+	+
YNL096C	RPS7B	42	+	+	+
YNL178W	RPS3	47	+	+	+
YNL301C	RPL18B	41	+	+	+
YNL302C	RPS19B	50	+	+	+
YOL039W	RPP2A	43	+	+	+
YOL127W	RPL25	49	+	+	+
YOR063W	RPL3	58	+	+	+
YOR096W	RPS7A	41	+	+	+
YOR204W	DED1	17	+	+	+
YOR234C	RPL33B	58	+	+	+
YOR369C	RPS12	47	+	+	+
YPL131W	RPL5	43	+	+	+
Membrane trafficking					
YLR447C	VMA6	28	+	+	+
YDL113C	ATG20	42	+	+	+
YGL008C	PMA1	21	+	+	+
YBR127C	VMA2	35	+	+	+
Unknown					
YAR073W	IMD1	19	+	+	+

Chapter 4: Conclusions and Future Directions

The discovery of replication checkpoint and its essential role in maintaining genomic integrity has been appreciated for decades. Studies in yeast species have advanced our knowledge about the major players in this pathway and how they function to couple different cellular processes in response to replication stress, in particular the effector kinases. The work described in this dissertation is based on an in vitro assay for quantitative measurement of effector kinase, Dun1's activities. This approach has led us to determine the key phosphorylation event for its activation by reconstituting the phosphorylation state of Dun1. We provided evidence supporting that this key phosphorylation event on the activation loop of Dun1 is conserved across all Chk2 family kinases, including Rad53, another effector kinase in replication checkpoint in budding yeast. Furthermore, these studies on Dun1 activation suggested a reconstitution system consisting of Dun1 and Sml1 could amplify the signal of Dun1 activity by more than a thousand fold. Since the only activator of Dun1 is Rad53, I reasoned this reconstituted system could serve as a sensitive system to screen for any activator for Rad53 activity.

There are dozens of proteins that have been implicated in Rad53 activation. Only two adaptor proteins, Rad9 and Mrc1 have been shown to directly associate with Rad53. As a result, I decided to test if adaptor proteins or their associated factors could trigger Rad53 activation. By utilizing a reconstituted Rad53-Dun1-Sml1 system, Mrc1 showed a stimulating effect in

activating Rad53 by Mec1. I further demonstrated this effect using purified proteins. Kinetic analysis showed that instead of a two-step linear pathway, the primary role of Mrc1 is to promote Rad53 phosphorylation by Mec1 by catalyzing the enzyme-substrate interaction between Mec1 and Rad53.

Implication from my studies on the association between adaptor protein Mrc1 with upstream kinase Mec1 could be a essential regulation for effector kinase activation. Upon replication stress, the first mode of regulation is the recruitment of proteins including Mec1 to stalled replication forks. The relocalization of Mec1 makes it concentrated and closer to Mrc1. While numerous proteins are localized to replication forks, it is possible that a second mode of regulation is through this intrinsic association between Mec1 and Mrc1. This specific intrinsic association could promote Mrc1's phosphorylation by Mec1, recruitment of Rad53, and Rad53 phosphorylation by Mec1. This study thus provides mechanistic insights into the role of adaptor proteins for DNA replication checkpoint activation.

This dissertation has laid the foundation to understand the activation of effector kinases with a very specific reconstituted system. Since there are many proteins involved in Rad53 activation, by utilizing this system, we can gradually untangle the role of different proteins in activating Rad53 in addition to Mrc1 and Mec1. For example, the mechanism of how direct Sgs1

association with Rad53 involved in Rad53 activation other than its specific process of DNA by Sgs1. A candidate approach of Rad53 activators applying to this in vitro reconstitution system could provide direct mechanistic insights into different regulations of Rad53 activation.

Mec1 is a 270 kilo-dalton protein that is composed of several functional domains. A systematic analysis in dissecting the region where Mec1 associates with Mrc1 will be challenging but crucial in further understanding the functional importance of the association between Mrc1 and Mec1 in vivo.

DNA plays an essential role in the activation of checkpoint. In our reconstituted system, no DNA is present. It will be important to further couple the in vitro and vivo relevance if different DNA structures together with proteins including RPA, Mrc1, Mec1 and others are tested for their effects on the activation of Rad53.

References

Alcasabas, A.A., Osborn, A.J., Bachant, J., Hu, F., Werler, P.J., Bousset, K., Furuya, K., Diffley, J.F., Carr, A.M., and Elledge, S.J. (2001). Mrc1 transduces signals of DNA replication stress to activate Rad53. Nat Cell Biol *3*, 958-965.

Araki, H., Leem, S.H., Phongdara, A., and Sugino, A. (1995). Dpb11, which interacts with DNA polymerase II(epsilon) in Saccharomyces cerevisiae, has a dual role in S-phase progression and at a cell cycle checkpoint. Proc Natl Acad Sci U S A *92*, 11791-11795.

Bashkirov, V.I., Bashkirova, E.V., Haghnazari, E., and Heyer, W.D. (2003). Direct kinase-to-kinase signaling mediated by the FHA phosphoprotein recognition domain of the Dun1 DNA damage checkpoint kinase. Mol Cell Biol *23*, 1441-1452.

Bjergbaek, L., Cobb, J.A., Tsai-Pflugfelder, M., and Gasser, S.M. (2005). Mechanistically distinct roles for Sgs1p in checkpoint activation and replication fork maintenance. Embo J *24*, 405-417.

Chen, S.H., Smolka, M.B., and Zhou, H. (2007). Mechanism of Dun1 activation by Rad53 phosphorylation in Saccharomyces cerevisiae. J Biol Chem *282*, 986-995.

Desany, B.A., Alcasabas, A.A., Bachant, J.B., and Elledge, S.J. (1998). Recovery from DNA replicational stress is the essential function of the S-phase checkpoint pathway. Genes Dev *12*, 2956-2970.

Emili, A. (1998). MEC1-dependent phosphorylation of Rad9p in response to DNA damage. Mol Cell *2*, 183-189.

Foss, E.J. (2001). Tof1p regulates DNA damage responses during S phase in Saccharomyces cerevisiae. Genetics *157*, 567-577.

Gambus, A., Jones, R.C., Sanchez-Diaz, A., Kanemaki, M., van Deursen, F., Edmondson, R.D., and Labib, K. (2006). GINS maintains association of Cdc45

with MCM in replisome progression complexes at eukaryotic DNA replication forks. Nat Cell Biol *8*, 358-366.

Garcia, V., Furuya, K., and Carr, A.M. (2005). Identification and functional analysis of TopBP1 and its homologs. DNA Repair (Amst) *4*, 1227-1239.

Gardner, R., Putnam, C.W., and Weinert, T. (1999). RAD53, DUN1 and PDS1 define two parallel G2/M checkpoint pathways in budding yeast. Embo J *18*, 3173-3185.

Gilbert, C.S., Green, C.M., and Lowndes, N.F. (2001). Budding yeast Rad9 is an ATP-dependent Rad53 activating machine. Mol Cell *8*, 129-136.

Guo, Z., Kumagai, A., Wang, S.X., and Dunphy, W.G. (2000). Requirement for Atr in phosphorylation of Chk1 and cell cycle regulation in response to DNA replication blocks and UV-damaged DNA in Xenopus egg extracts. Genes Dev *14*, 2745-2756.

Hartwell, L.H., and Kastan, M.B. (1994). Cell cycle control and cancer. Science *266*, 1821-1828.

Ho, Y., Gruhler, A., Heilbut, A., Bader, G.D., Moore, L., Adams, S.L., Millar, A., Taylor, P., Bennett, K., Boutilier, K.*, et al.* (2002). Systematic identification of protein complexes in Saccharomyces cerevisiae by mass spectrometry. Nature *415*, 180-183.

Hodgson, B., Calzada, A., and Labib, K. (2007). Mrc1 and Tof1 regulate DNA replication forks in different ways during normal S phase. Mol Biol Cell *18*, 3894-3902.

Huang, M., Zhou, Z., and Elledge, S.J. (1998). The DNA replication and damage checkpoint pathways induce transcription by inhibition of the Crt1 repressor. Cell *94*, 595-605.

Jackson, S.P. (1996). The recognition of DNA damage. Curr Opin Genet Dev *6*, 19-25.

Johnson, L.N., Noble, M.E., and Owen, D.J. (1996). Active and inactive protein kinases: structural basis for regulation. Cell *85*, 149-158.

Kamimura, Y., Masumoto, H., Sugino, A., and Araki, H. (1998). Sld2, which interacts with Dpb11 in Saccharomyces cerevisiae, is required for chromosomal DNA replication. Mol Cell Biol *18*, 6102-6109.

Katou, Y., Kanoh, Y., Bando, M., Noguchi, H., Tanaka, H., Ashikari, T., Sugimoto, K., and Shirahige, K. (2003). S-phase checkpoint proteins Tof1 and Mrc1 form a stable replication-pausing complex. Nature *424*, 1078-1083.

Kumagai, A., Kim, S.M., and Dunphy, W.G. (2004). Claspin and the activated form of ATR-ATRIP collaborate in the activation of Chk1. J Biol Chem *279*, 49599-49608.

Kumagai, A., Lee, J., Yoo, H.Y., and Dunphy, W.G. (2006). TopBP1 activates the ATR-ATRIP complex. Cell *124*, 943-955.

Lee, C.H., and Chung, J.H. (2001). The hCds1 (Chk2)-FHA domain is essential for a chain of phosphorylation events on hCds1 that is induced by ionizing radiation. J Biol Chem *276*, 30537-30541.

Lee, J., Kumagai, A., and Dunphy, W.G. (2007). The Rad9-Hus1-Rad1 checkpoint clamp regulates interaction of TopBP1 with ATR. J Biol Chem *282*, 28036-28044.

Lee, S.J., Schwartz, M.F., Duong, J.K., and Stern, D.F. (2003). Rad53 phosphorylation site clusters are important for Rad53 regulation and signaling. Mol Cell Biol *23*, 6300-6314.

Lee, Y.D., and Elledge, S.J. (2006). Control of ribonucleotide reductase localization through an anchoring mechanism involving Wtm1. Genes Dev *20*, 334-344.

Longtine, M.S., McKenzie, A., 3rd, Demarini, D.J., Shah, N.G., Wach, A., Brachat, A., Philippsen, P., and Pringle, J.R. (1998). Additional modules for versatile and economical PCR-based gene deletion and modification in Saccharomyces cerevisiae. Yeast *14*, 953-961.

Lopes, M., Cotta-Ramusino, C., Pellicioli, A., Liberi, G., Plevani, P., Muzi-Falconi, M., Newlon, C.S., and Foiani, M. (2001). The DNA replication checkpoint response stabilizes stalled replication forks. Nature *412*, 557-561.

Lou, H., Komata, M., Katou, Y., Guan, Z., Reis, C.C., Budd, M., Shirahige, K., and Campbell, J.L. (2008). Mrc1 and DNA polymerase epsilon function together in linking DNA replication and the S phase checkpoint. Mol Cell *32*, 106-117.

Ma, J.L., Lee, S.J., Duong, J.K., and Stern, D.F. (2006). Activation of the checkpoint kinase Rad53 by the phosphatidyl inositol kinase-like kinase Mec1. J Biol Chem *281*, 3954-3963.

Majka, J., and Burgers, P.M. (2003). Yeast Rad17/Mec3/Ddc1: a sliding clamp for the DNA damage checkpoint. Proc Natl Acad Sci U S A *100*, 2249-2254.

Majka, J., Niedziela-Majka, A., and Burgers, P.M. (2006). The checkpoint clamp activates Mec1 kinase during initiation of the DNA damage checkpoint. Mol Cell *24*, 891-901.

Matsuoka, S., Rotman, G., Ogawa, A., Shiloh, Y., Tamai, K., and Elledge, S.J. (2000). Ataxia telangiectasia-mutated phosphorylates Chk2 in vivo and in vitro. Proc Natl Acad Sci U S A *97*, 10389-10394.

Mordes, D.A., Glick, G.G., Zhao, R., and Cortez, D. (2008). TopBP1 activates ATR through ATRIP and a PIKK regulatory domain. Genes Dev *22*, 1478-1489.

Morrison, A., Araki, H., Clark, A.B., Hamatake, R.K., and Sugino, A. (1990). A third essential DNA polymerase in S. cerevisiae. Cell *62*, 1143-1151.

Myung, K., Datta, A., and Kolodner, R.D. (2001). Suppression of spontaneous chromosomal rearrangements by S phase checkpoint functions in Saccharomyces cerevisiae. Cell *104*, 397-408.

Navadgi-Patil, V.M., and Burgers, P.M. (2008). Yeast DNA replication protein Dpb11 activates the Mec1/ATR checkpoint kinase. J Biol Chem.

Navas, T.A., Zhou, Z., and Elledge, S.J. (1995). DNA polymerase epsilon links the DNA replication machinery to the S phase checkpoint. Cell *80*, 29-39.

Neecke, H., Lucchini, G., and Longhese, M.P. (1999). Cell cycle progression in the presence of irreparable DNA damage is controlled by a Mec1- and Rad53-dependent checkpoint in budding yeast. Embo J *18*, 4485-4497.

Nyberg, K.A., Michelson, R.J., Putnam, C.W., and Weinert, T.A. (2002). Toward maintaining the genome: DNA damage and replication checkpoints. Annu Rev Genet *36*, 617-656.

Osborn, A.J., and Elledge, S.J. (2003). Mrc1 is a replication fork component whose phosphorylation in response to DNA replication stress activates Rad53. Genes Dev *17*, 1755-1767.

Pan, X., Ye, P., Yuan, D.S., Wang, X., Bader, J.S., and Boeke, J.D. (2006). A DNA integrity network in the yeast Saccharomyces cerevisiae. Cell *124*, 1069-1081.

Samadashwily, G.M., Raca, G., and Mirkin, S.M. (1997). Trinucleotide repeats affect DNA replication in vivo. Nat Genet *17*, 298-304.

Sanchez, Y., Desany, B.A., Jones, W.J., Liu, Q., Wang, B., and Elledge, S.J. (1996). Regulation of RAD53 by the ATM-like kinases MEC1 and TEL1 in yeast cell cycle checkpoint pathways. Science *271*, 357-360.

Santocanale, C., and Diffley, J.F. (1998). A Mec1- and Rad53-dependent checkpoint controls late-firing origins of DNA replication. Nature *395*, 615-618.

Schwartz, M.F., Duong, J.K., Sun, Z., Morrow, J.S., Pradhan, D., and Stern, D.F. (2002). Rad9 phosphorylation sites couple Rad53 to the Saccharomyces cerevisiae DNA damage checkpoint. Mol Cell *9*, 1055-1065.

Smolka, M., Albuquerque, SP., Chen, SH., Schmidt, KH., Wei, XX., Kolodner, RD. and Zhou, H. (2005). Dynamic Changes in Protein-protein Interaction and Protein Phosphorylation Probed with Amine Reactive Isotope Tag. Molecular and Cellular Proteomics *4*, 1358-1369.

Sogo, J.M., Lopes, M., and Foiani, M. (2002). Fork reversal and ssDNA accumulation at stalled replication forks owing to checkpoint defects. Science *297*, 599-602.

Sun, Z., Fay, D.S., Marini, F., Foiani, M., and Stern, D.F. (1996). Spk1/Rad53 is regulated by Mec1-dependent protein phosphorylation in DNA replication and damage checkpoint pathways. Genes Dev *10*, 395-406.

Sun, Z., Hsiao, J., Fay, D.S., and Stern, D.F. (1998). Rad53 FHA domain associated with phosphorylated Rad9 in the DNA damage checkpoint. Science *281*, 272-274.

Sweeney, F.D., Yang, F., Chi, A., Shabanowitz, J., Hunt, D.F., and Durocher, D. (2005). Saccharomyces cerevisiae Rad9 acts as a Mec1 adaptor to allow Rad53 activation. Curr Biol *15*, 1364-1375.

Szyjka, S.J., Viggiani, C.J., and Aparicio, O.M. (2005). Mrc1 is required for normal progression of replication forks throughout chromatin in S. cerevisiae. Mol Cell *19*, 691-697.

Tanaka, K., Boddy, M.N., Chen, X.B., McGowan, C.H., and Russell, P. (2001). Threonine-11, phosphorylated by Rad3 and atm in vitro, is required for activation of fission yeast checkpoint kinase Cds1. Mol Cell Biol *21*, 3398-3404.

Tanaka, K., and Russell, P. (2001). Mrc1 channels the DNA replication arrest signal to checkpoint kinase Cds1. Nat Cell Biol *3*, 966-972.

Tercero, J.A., and Diffley, J.F. (2001). Regulation of DNA replication fork progression through damaged DNA by the Mec1/Rad53 checkpoint. Nature *412*, 553-557.

Tercero, J.A., Longhese, M.P., and Diffley, J.F. (2003). A central role for DNA replication forks in checkpoint activation and response. Mol Cell *11*, 1323-1336.

Tourriere, H., Versini, G., Cordon-Preciado, V., Alabert, C., and Pasero, P. (2005). Mrc1 and Tof1 promote replication fork progression and recovery independently of Rad53. Mol Cell *19*, 699-706.

Uchiki, T., Dice, L.T., Hettich, R.L., and Dealwis, C. (2004). Identification of phosphorylation sites on the yeast ribonucleotide reductase inhibitor Sml1. J Biol Chem *279*, 11293-11303.

Vialard, J.E., Gilbert, C.S., Green, C.M., and Lowndes, N.F. (1998). The budding yeast Rad9 checkpoint protein is subjected to Mec1/Tel1-dependent hyperphosphorylation and interacts with Rad53 after DNA damage. Embo J *17*, 5679-5688.

Wang, H., and Elledge, S.J. (2002). Genetic and physical interactions between DPB11 and DDC1 in the yeast DNA damage response pathway. Genetics *160*, 1295-1304.

Watt, P.M., Hickson, I.D., Borts, R.H., and Louis, E.J. (1996). SGS1, a homologue of the Bloom's and Werner's syndrome genes, is required for maintenance of genome stability in Saccharomyces cerevisiae. Genetics *144*, 935-945.

Weinert, T.A., Kiser, G.L., and Hartwell, L.H. (1994). Mitotic checkpoint genes in budding yeast and the dependence of mitosis on DNA replication and repair. Genes Dev *8*, 652-665.

Xu, Y.J., Davenport, M., and Kelly, T.J. (2006). Two-stage mechanism for activation of the DNA replication checkpoint kinase Cds1 in fission yeast. Genes Dev *20*, 990-1003.

Zhang, Z., An, X., Yang, K., Perlstein, D.L., Hicks, L., Kelleher, N., Stubbe, J., and Huang, M. (2006). Nuclear localization of the Saccharomyces cerevisiae ribonucleotide reductase small subunit requires a karyopherin and a WD40 repeat protein. Proc Natl Acad Sci U S A *103*, 1422-1427.

Zhao, X., Chabes, A., Domkin, V., Thelander, L., and Rothstein, R. (2001). The ribonucleotide reductase inhibitor Sml1 is a new target of the Mec1/Rad53 kinase cascade during growth and in response to DNA damage. Embo J *20*, 3544-3553.

Zhao, X., Muller, E.G., and Rothstein, R. (1998). A suppressor of two essential checkpoint genes identifies a novel protein that negatively affects dNTP pools. Mol Cell *2*, 329-340.

Zhao, X., and Rothstein, R. (2002). The Dun1 checkpoint kinase phosphorylates and regulates the ribonucleotide reductase inhibitor Sml1. Proc Natl Acad Sci U S A *99*, 3746-3751.

Zhou, Z., and Elledge, S.J. (1993). DUN1 encodes a protein kinase that controls the DNA damage response in yeast. Cell *75*, 1119-1127.

Zou, L., and Elledge, S.J. (2003). Sensing DNA damage through ATRIP recognition of RPA-ssDNA complexes. Science *300*, 1542-1548.